

# **The Development of Nano-Composite Polysulphone Membranes with Reduced Fouling Properties for use in Wastewater Treatment**

Report to the  
**Water Research Commission**

by

**Prof Priscilla G L Baker, Heidi L Richards, Lisebo Phelane, Emmanuel I Iwuoha**  
SensorLab, Chemistry Department, University of the Western Cape

**WRC Report No. 2006/1/14**  
**ISBN 978-1-4312-0609-4**

**December 2014**

**Obtainable from**

Water Research Commission  
Private Bag X03  
Gezina, 0031

[orders@wrc.org.za](mailto:orders@wrc.org.za) or download from [www.wrc.org.za](http://www.wrc.org.za)

**DISCLAIMER**

This report has been reviewed by the Water Research Commission (WRC) and approved for publication. Approval does not signify that the contents necessarily reflect the views and policies of the WRC, nor does mention of trade names or commercial products constitute endorsement or recommendation for use.

## EXECUTIVE SUMMARY

### BACKGROUND

Many studies have been conducted to increase the hydrophilic properties of the polysulphone membrane surface. These studies can be divided into three categories: 1) blending PSF with hydrophilic nanoparticles such as  $\text{SiO}_2$ ,  $\text{ZrO}_2$  and  $\text{TiO}_2$ , 2) grafting with hydrophilic polymers, monomers or functional groups and 3) coating with hydrophilic polymers (Yanan et al. 2007). Of the aforementioned methods, blending with nanoparticles has attracted much interest in the past 10 years due to their convenient operation and mild conditions. Blending offers the advantage for the preparation of artificial membranes with excellent separation performance, good thermal and chemical resistance and adaptability to the harsh wastewater environments (Maximous et al. 2009). In recent years, various metal nanoparticles have been used in wastewater treatment membrane technology with varied success. Previous studies have investigated the effectiveness of  $\text{TiO}_2$ ,  $\text{Al}_2\text{O}_3$ , Ag,  $\text{Fe}_3\text{O}_4$  and most recently  $\text{ZrO}_2$  nanoparticles as membrane filler for the treatment of wastewater (Zodrow et al. 2009). These metal centres act as redox mediators to reduce hydrophobicity of the membrane.

Nanocomposite membranes are attractive for the purpose of creating new materials with enhanced properties such as high perm selectivity, good hydrophilicity and excellent fouling resistance. Taurozzi et al. summarized the effect of nanoparticles on membrane performance in general. These included increased membrane thickness, higher surface porosity and higher permeability of the membrane. The main objective however for using nanoparticles was often to reduce fouling (Kim, Van der Bruggen 2010). Studies of blending membranes with nanoparticles have focused primarily on gas separation and pervaporation membranes and have only recently been extended to porous membranes for ultrafiltration and potential nanofiltration applications (Maximous et al. 2009). Nanocomposite membranes can remediate two types of fouling: membrane fouling due to organic matter and biofouling. Titanium nanoparticles have mostly been used to mitigate the former. Li et al. showed that water flux through a polyethersulfone- $\text{TiO}_2$  membrane was significantly enhanced, but the effect was concentration dependent. This is due to nanoparticle agglomeration (Kim, Van der Bruggen 2010). Other studies have however contradicted this finding (Yanan et al. 2007) and it must therefore be noted that different findings may arise from differences in procedures and materials.

The use of hydrogels as ultrafiltration-type membranes could be considered, but unfortunately these polymers do not have the mechanical properties to act as such membranes by themselves. Currently hydrogels are being investigated as hydrophilic surface coating layer to hydrophobic PSF membranes. In ideal circumstances, such a coating layer should increase fouling resistance without markedly compromising the water flux through the membrane (Bae, Tak 2005). This approach to membrane synthesis is called a composite membrane approach, combining the preparation of a porous mechanical support with a coating layer that has tailored properties to control sieving, permeation and surface chemistry. Poly (ethylene glycol) (PEG) and PEG-based materials have been proven to be excellent coatings for PSF membranes due to their amphiphilic nature, biocompatibility and excellent resistance to non-specific protein and other macromolecules adhesion. This area of research is very new and could hold the key to developing an anti-fouling membrane for use in wastewater purification

## **RATIONALE**

Polysulphone (PSF) membranes are the most common membranes used in ultrafiltration of wastewater due to its mechanical robustness and structural- and chemical stability. Unfortunately PSF is a hydrophobic material, making its surface prone to fouling due to adsorptive mechanisms. Many studies have been conducted to increase the hydrophilic properties of the polysulphone membrane surface. Hydrophilicity of membranes refers to the charge-polarized properties of the membrane material and its capacity for hydrogen bonding. Hydrophilic and hydrophobic molecules are also known as polar molecules and nonpolar molecules, respectively. For instance, a hydrophilic membrane will not be fouled with oil, grease or other hydrophobic substances. The membrane is highly attractive to water so the water molecules will push away other molecules in order to gain access to the membrane. Once formed, hydrogen bonds are quite stable and reluctant to break apart. This keeps contaminants away from the membrane so it remains clean and functioning for longer.

In this work, two divergent approaches in materials synthesis were incorporated to produce polysulfone membrane materials that would be suitable for membrane development and water treatment applications. The first strategy involved the preparation of well defined; metal nanoparticle modified homogeneous polysulfone membranes, based on dispersion of chemically synthesised metal nanoparticles within polysulfone thin films. The metal nanoparticles used in the study were selected for their documented catalytic properties.

However, presently there is a strong awareness of the need to assess the eco-toxicity of any method or technology that may potentially release nanoparticles into air, water, food or health domain. Hence a second synthetic strategy that does not involve metal nanoparticles was also identified. The second synthetic strategy involved the chemical synthesis of chemically cross linked hydrogels with improved hydrophobicity for improved separation as well as the necessary mechanical strength for membrane development and application. The polysulfone hydrogel synthesis, surface properties and analytical response to selected model compounds was carefully evaluated.

The research programme was designed to facilitate capacity building in the field of designing and preparation of novel polymer composites with the desired characteristics for water treatment applications, to demonstrate the suitability of electrochemical methods as analytical tools to evaluate membrane materials and to demonstrate membrane performance capacity in laboratory scale experiments. The laboratory scale experiments were developed from a literature precedent identifying major fouling processes, following a recommendation from the steering committee group.

Natural organic matter (NOM) is known to be the worst foulant in the membrane processes, but the complexities of NOM make it difficult to determine its effects on membrane fouling. Therefore, simple organic compounds (surrogates for NOM) are used in research to investigate the fouling mechanisms in ultrafiltration. Previous research on NOM components in membrane processes indicated that polysaccharides formed an important part of the fouling cake. From literature the NOM components are made up of polysaccharides (e.g. dextran, alginic acid, and polygalacturonic acid) and small carbohydrates (e.g. tannic acid) were evaluated for their removal in softening (the treatment process in the City of Austin). (Kweon et al. 2005) For the purpose of quantitative evaluation of membrane transport

properties and analytical performance by electrochemical methods, we have selected alginic acid and tannic acid as target molecules.

## **OBJECTIVES AND AIMS**

### **Objective 1: Evaluation of the status quo of polysulfone modification by metal nanoparticle incorporation**

#### **AIM 1**

Comprehensive literature review on metal nanoparticle modified polysulfone membranes and its application in water treatment, with careful attention to the modifications effected to improve fouling properties of the modified membrane systems.

### **Objective 2: Synthesis and characterisation of novel polysulfone composites with reduced hydrophobicity**

#### **AIM 2**

Synthesis of polysulphone thin films modified with Co and Ni nanoparticles by chemical and electrochemical methods from readily available laboratory reagents and optimising synthesis conditions. The chemically synthesised polysulphone (PSF) material will be evaluated in terms of processability of the material and fundamental electrochemistry.

#### **AIM 3**

Modification of the PSF membrane by chemical crosslinking to produce polysulfone hydrogels, followed by spectroscopic and morphological characterisation of the modified PSF materials will be done. The effect of PSF contribution on hydrophilicity and morphology will be evaluated.

### **Objective 3: Analytical response of polysulfone nanocomposites using model organic compounds in laboratory scale experiments.**

#### **AIM 4**

The analytical response of polysulfone composites and hydrogels will be evaluated as concentration dependent chemical sensor response in the presence of model organic compounds. The fouling ability will be assessed in terms of sensitivity of the membranes to individual compounds and the time to passivation of the membrane material.

## **RESULTS AND DISCUSSION**

### **Aim 1**

A comprehensive literature review on metal nanoparticle modified polysulfone membranes was done to assess the advances and progress in terms of incorporation of metal nanoparticles into polysulfones. The literature review identified that several strategies for using metal nanoparticles as modifiers in polymer matrices had been investigated in the past 5-10 years. In polymeric membranes nanoparticles are used as additives in the synthesis procedure or *in situ* generated, to allow a high degree of control over membrane characteristics as well as the ability to produce ceramic membranes in the nanofiltration membrane range. The review also identified the need for better understanding of the membrane fouling with nanoparticle-enhanced membranes in water and waste water treatment is still lacking, since fouling is strongly dependent on the physicochemical aspects

of nanoparticles such as particle size, hydrophilicity and surface charge. The need for further research in this area was highlighted as a combination of the effects of water chemistry, nature of nanoparticles on membrane performance.

*Publication:* **Journal of Surface Engineered Materials and Advanced Technology**, 2012, 2, 183-193. Metal Nanoparticle Modified Polysulfone Membranes for Use in Wastewater Treatment: A Critical Review; Heidi L Richards, Priscilla G. L. Baker, Emmanuel I Iwuoha.  
**Downloads: 1527 times**

## **Aim 2**

The chemically synthesised polysulphone (PSF) material and incorporation of metal nanoparticles was evaluated in terms of processability of the material and fundamental electrochemistry, surface characterisation and fundamental electrochemistry in the presence of convection. Free metal of Co and Ni were synthesised by reduction of the corresponding metal salts to produce nanoparticles in a suspension. The metal particles were confirmed to be in the nanometer range by high resolution SEM evaluation. Energy dispersive X-ray analysis confirmed that PSF/nanoparticle composites contained the Co and Ni nanoparticles respectively, uniformly dispersed in the drop coated thin films. The TEM images of Ni nanoparticles confirmed a cubic shape, favouring the face centered cubic crystalline form of Ni nanoparticle, which has very high (74%) packing efficiency which supports the observation of smallest pore sizes (0.5-1.5  $\mu\text{m}$ ) from SEM. Thus demonstrating that the simple chemical synthesis approach could produce thin films of PSF/Co and PSF/Ni at ambient conditions at minimal cost.

The diffusion coefficient of PSF, PSF/Co and PSF/Ni thin films were evaluated by cyclic voltammetry in  $\text{H}_2\text{SO}_4$  (for aqueous applications) and phosphate buffer (for potential biosensor applications), using  $\text{K}_3\text{Fe}(\text{CN})_6$  as redox probe (Table A1).

The highest electron mobility as evaluated by diffusion coefficient calculated from Randles Sevcik plots was determined for PSF/Ni thin films. PSF/Ni films also showed the greatest increase in porosity confirmed by SEM and AFM. In the presence of  $\text{K}_3\text{Fe}(\text{CN})_6$  the diffusion coefficient is an indication of the rate at which  $\text{Fe}^{2+}/\text{Fe}^{3+}$  ions are brought to the membrane surface, during the redox cycling and the PSF/Ni film consistently produced higher diffusion coefficients. Introducing convection by rotating the working electrode at controlled rotation speed and evaluating the diffusion coefficients confirmed that the reversible electrochemistry was enhanced at rotation speeds up to 200 rpm, although capacitive behaviour increased as a function of the rotation speed. Diffusion coefficients were comparable for electron mobility (absence of redox probe) as well as for ion diffusion (in the presence of  $\text{K}_3\text{Fe}(\text{CN})_6$ ) (Table A2).

The diffusion properties of cellulose acetate (commercial hydrophilic membrane) and polyethersulfone (commercial hydrophobic membrane) under similar conditions, could not be established since the suppliers could not verify the concentration of the stock solution provided. However contact angle measurement and wettability tests placed the performance of the PSF/Co and PSF/Ni thin films close to that of the hydrophilic cellulose acetate films, prepared by drop coating.

Contact angle measurement confirmed that the incorporation of metal nanoparticles as redox centres effectively reduced hydrophobicity by 50% compared to unmodified polysulfone (Table A3). This was also confirmed by simple wetting experiments with pure water (Figure A1).

*Output:* Phelane L, Muya F N., Richards H. L, Baker P G.L, Iwuoha E, (2013). Polysulfone Nanocomposite Membranes with improved hydrophilicity. **Electrochimica Acta** (2014). Online at <http://dx.doi.org/10.1016/j.electacta.2013.11.156>

### AIM 3

Modification of the PSF membrane by chemical crosslinking to produce polysulfone hydrogels, followed by spectroscopic and morphological characterisation of the modified PSF materials will be done. The effect of PSF contribution on hydrophilicity and morphology will be evaluated.

Hydrogels were prepared by reflux at controlled temperature. PSF-PVA hydrogels were synthesised by dissolving 0.4421 g of polysulfone crystals into 50 mL of N,N-dimethylacetamide (DMAc) to produce 0.0554 M PSF-solution after 1 hour of sonication. 5 mL of this solution was transferred to a round bottom flask, to which 2.5895g of PVA was added. To the mixture 1 mL glutaraldehyde cross-linker solution was added, followed by the catalyst in order to speed up the reaction during the crosslinking process. An excess of acid was required for protonation and reduction of the aldehyde into alcohol. 1 mL of 2 M HCl catalyst was added the reflux mixture and the mixture was allowed to for 3 hours at 75°C with constant stirring. The resultant hydrogel was allowed to age for 10 days after which an electrochemically and chemically stable hydrogel was produced.

The starting materials and polysulfone hydrogels respectively, were all evaluated by FTIR, SEM, AFM and electrochemical methods (CV, SWV, RDE and EIS) in order to confirm the crosslinking chemistry and evaluate the interfacial kinetic behaviour related to solution transport properties.

Thin films of the starting polymers as well as the hydrogel composites were prepared by drop coating 10  $\mu\text{L}$  aliquot of the solution onto a glassy carbon electrode (GCE) with a micropipette and left to dry overnight before analysis. Electrochemically characterization was performed by cycling the potential between -200 mV and +1200 mV in HCl, at scan rates ranging from 10 to 300  $\text{mV.s}^{-1}$ . The platinum (Pt) counter electrode was regularly cleaned before and after synthesis.

The cross linking of PVA and PSF at three different ratios i.e. 25:75, 50:50 and 75:25, produced three unique hydrogels materials, which were characterised using spectroscopy, morphology and electrochemistry techniques. Hydrogels performance in the presence of target molecule was evaluated by hydrodynamic voltammetry, and electrochemical impedance spectroscopy. Surface roughness evaluated from AFM calculations showed a distribution of roughness associated with PSF percentage contribution. Surface roughness increased from 155.5 nm for unmodified PSF up to 769.8 nm for hydrogel depending on the hydrogel composition. Surface roughness could be associated with hydrophilicity and showed good correlation with contact angle data as well as diffusion coefficient data.

The contact angle of the unmodified polysulfone membrane was 103° and upon modification with hydrophilic polymer (PVA) contact angle decreased to as low as 36°, depending on hydrogel composition. High surface roughness was linked to improved hydrophilicity and was also shown to agree with improved electron mobility within the polymer matrix. Crosslinking PSF with (PVA) reduced the hydrophobic nature of PSF as evidenced by surface features such as shape and size distribution as well as surface roughness. Crosslinking PSF and PVA also improved electron transfer properties (Table A5).

However, we also observed that the hydrogel composition did not vary significantly when changing the contribution of each polymer in the crosslinking chemistry. The presence of a hydrophilic polymer chemically fixed by crosslinking, produced a reproducible hydrogel with greatly reduced hydrophilicity. The analytical response of the hydrogels in the presence of model compounds were evaluated at low concentration (before the onset of fouling) to assess the interfacial kinetics associated with the analyte redox performance.

*Output:* Synthesis and characterisation of polysulfone hydrogels; Francis N Muya, Lisebo Phelane, E I Iwuoha and Priscilla GL Baker. **Journal of surface engineered material and advanced technology** (Paper ID: 1180218, Accepted 27 February 2014).

#### **AIM 4**

The analytical response of polysulfone composites and hydrogels will be evaluated as concentration dependent chemical sensor response in the presence of model organic compounds. The fouling ability will be assessed in terms of sensitivity of the membranes to individual compounds and the time to passivation of the membrane material.

Effect of a change in analyte concentration at fixed scan rate and fixed rotation speed was used to assess fouling behaviour under hydrodynamic conditions. Fouling is the accumulation of unwanted material on solid surfaces to the detriment of function. Similar trends in analytical performance were observed by cyclic voltammetry (quiet solutions) as for rotating disk electrochemistry (hydrodynamic conditions). Tannic acid showed catalytic oxidation at the hydrogel interfaces whereas alginic acid oxidation followed an adsorptive reaction mechanism. The analytical response of dominant PSF hydrogel (75:25) was observed to be most sensitive towards quantitative detection of both tannic and alginic acid (Table A6 and A7).

Under hydrodynamic conditions 75:25 hydrogel maintained its superior performance, even though the linear range for concentration dependence, was reduced (Table A8). Analytical response was maintained at convection speeds up to 200 rpm. The dynamic linear range measured for all three hydrogels was established to be similar. All hydrogels showed good linear response and comparable sensitivity to the model compounds, with onset of fouling behaviour at around 6 µM (Table A8).

*Output:* Hydrophilic polysulfone chemical sensors for small organic molecules” by authors Lisebo Phelane, Francis N Muya, Priscilla GL Baker, Emmanuel Iwuoha. Invited for publication and **submitted** February 2014. **Special issue of Electrochimica Acta** dedicated to papers from 64th Annual meeting of International Society of Electrochemistry, 8-13 September, 2013, Santiago de Queretaro, Mexico.



## **GENERAL**

We have demonstrated the successful synthesis of hydrophilic polysulfone derivatives from simple chemical precursors commercially available from local chemical suppliers. Two approaches for synthesis of reproducible thin films of hydrophilic polysulfone have been analysed in detail in order to understand the underlying mechanisms that govern the improvement in surface mass transport properties.

The hydrophilic polysulfone materials have been characterised extensively in an attempt to verify structure, physical and chemical properties of the novel polysulfone composite materials. Spectroscopic investigation was used to characterise the structure of the product and verify the efficiency of chemical modifications employed. Surface morphology analysis and electron microscopy was used to evaluate pore size and shape distribution of polysulfone composites, calculate size and shape of metal nanoparticles and confirm homogeneous incorporation of modifier in metal nanoparticle and hydrogel modified polysulfone materials. Electrochemistry was used to evaluate diffusional properties associated with conductivity of the polysulfone materials as thin film electrodes, evaluate their sensitivity towards selected analyte molecules and calculate their sensitivity to fouling at very low analyte concentration.

The polysulfone materials displayed improved mass transport properties in aqueous solutions and produced good linear response as chemical sensors to tannic acid and alginic acid in the micro molar concentration range. This sensitivity made it possible to determine the reaction mechanisms involved in mass transport of the model compounds in the presence and absence of convection, in a closed reaction vessel.

## **CONCLUSIONS**

Polysulfone modified with selected catalytic metal nanoparticles was successfully achieved. The polysulfone composite based on homogeneous incorporation of Ni nanoparticles, before film casting, was observed to have the smallest pore size and highest pore distribution per unit area. The Ni nanoparticles adopted the hexagonally close packed unit arrangement with packing efficiency up to 74%. In the analytical evaluation of PSF/Ni composites drop coated to form thin film chemical sensors, a very good sensitivity towards tannic acid and alginic acid was observed with a linear response in the micro molar concentration range.

One of the drawbacks of using metal nanoparticles in environmental applications relates to potential environmental health-related issues as a result of metal nanoparticles leaching into the environment. Hence a second synthetic approach was evaluated that does not involve metal nanoparticles, based on chemical crosslinking of polysulfone with a hydrophilic polymer to produce mechanically stable hydrophilic hydrogels. Polysulfone and polyvinyl alcohol were chemically cross linked using a short chain di-aldehyde to produce hydrogels with greatly reduced hydrophobicity, irrespective of the ratio of the starting polymers. All hydrogels showed similarities to the metal nanoparticle modified polysulfone in terms of surface morphology and electrochemical evaluation of mass transport properties to the thin film hydrogel surface in a three electrode arrangement. All hydrogel materials showed very good sensitivity and linear response to tannic acid and alginic acid at micro molar concentrations.

Overall the project has been successful in achieving all its objectives for materials design, development and testing at a laboratory scale. The project has provided skills training and expertise in advanced analytical methods for 1 PhD, 2 MSc and 2 Honours full time registered candidates (UWC). The data produced in this project has resulted in 3 peer reviewed publications in international scientific journals (already accepted) and a 4<sup>th</sup> full length research article submitted for peer review (February 2014).

## **RECOMMENDATIONS FOR FUTURE RESEARCH**

The research results show great promise for the utilisation of hydrophilic polysulfone derivatives for improved separation efficiency in aqueous media, as a direct consequence of reduced hydrophobicity at the interface of these membrane materials. The results at laboratory scale, small volume experiments bode well for efficient separation of polysaccharides and carbohydrates, as demonstrated by alginic acid and tannic acid response, respectively. It was demonstrated that alginic acid (polysaccharides) through adsorption mechanism posed a greater threat to membrane fouling as compared to tannic acid (carbohydrates). The research has also convincingly positioned electrochemistry as a reliable analytical technique for the evaluation of flux to membrane surfaces.

However to verify the fouling behaviour, a series of scaled-up experiments are necessary. The feasibility of casting flat membrane sheets using the polysulfone (Ni) and polysulfone cross linked with PVA (75:25) would have to be evaluated. The separation efficiency of these two membranes in a small volume flow through reaction cell has to be evaluated. The scaling up of the flow through volume would have to be evaluated as a function of membrane mechanical stability and separation efficiency.

Thereafter it is necessary to evaluate the membrane performance in a small scale membrane reactor using simulated separation mixtures as well as real organic membrane reactor feed solutions. This type of reaction vessel will facilitate evaluation of the efficiency of the membrane in the presence of physical foulants (sludge) and facilitate the evaluation of regenerating membranes *in situ*, using cost efficient regeneration processes. Electrochemical measurements and modelling of processes within the small scale membrane bio-reactor, will facilitate the demonstration of electrochemistry as an efficient analytical tool for the evaluation of flux through a membrane as well, following a well-developed literature precedent.

## ACKNOWLEDGEMENTS

The authors would like to thank the Reference Group of WRC Project K5/2006//3 for the assistance and the constructive discussions during the duration of the project:

The authors would also like to thank WRC for the investment in Kruss drop shape analysis system at University of the Western Cape, for the evaluation of surface energy, surface tension and contact angle in membrane analysis.

The authors sincerely appreciate the support and valuable discussions with the reference group of this project:

Prof Visvanathan Lin Pillay	University of Stellenbosch
Dr Enos Sitabule	Sasol Technology R&D
Mrs Ronel Augustyn	Sasol Technology R&D
Prof Rui Werner Krause	Rhodes University
Dr Wade Edwards	Atl-Hydro
Dr Jean-Francois Talbot	Talbot & Talbot (Pty) Ltd
Prof CA Buckley	University of KwaZulu-Natal

The authors also wish to acknowledge and appreciate the input support and guidance of the Research Manager Dr Valerie Naidoo as well as the administrative support of Mr Benny Mokgonyana.



## TABLE OF CONTENTS

EXECUTIVE SUMMARY .....	III
ACKNOWLEDGEMENTS.....	XI
TABLE OF CONTENTS.....	XIII
LIST OF FIGURES .....	XIV
LIST OF TABLES.....	XV
LIST OF ABBREVIATIONS .....	XVI
1 INTRODUCTION .....	1
1.1 Hydrophobicity vs hydrophilicity of membranes.....	1
1.2 Metal nanoparticle modified membranes.....	2
1.3 Hydrogels .....	5
2 EXPERIMENTAL .....	7
3 EXPERIMENTAL PROCEDURES .....	8
4 RESULTS AND TREATMENT OF DATA .....	11
5 CONCLUSIONS .....	35
6 RECOMMENDATIONS .....	36
7 LIST OF REFERENCES .....	37
APPENDIX:.....	39

## LIST OF FIGURES

- Figure 1: Structure of water showing charge interactions between water molecules
- Figure 2: HRTEM of Co nanoparticles
- Figure 3: EDX spectrum of the Co nanoparticles
- Figure 4: HRTEM of Ni nanoparticles
- Figure 5: EDX spectrum of Ni nanoparticles
- Figure 6: SEM of PSF
- Figure 7: SEM of PSF/Co
- Figure 8: SEM of PSF/Ni
- Figure 9: Raman spectrum of PSF
- Figure 10: Raman spectrum of PSF/Co
- Figure 11: Raman spectrum of PSF/Ni
- Figure 12: FTIR spectrum of PVA
- Figure 13: FTIR spectrum of polysulfone
- Figure 14: FTIR spectrum of 50:50 hydrogel
- Figure 15: SEM of (a) PSF unmodified and (b) 50:50 hydrogel (c) 75:25 hydrogel and (d) 25: 75 hydrogel
- Figure 16: Roughness distribution as measured from AFM data
- Figure 17 Contact angle distribution for hydrogel materials (a) as a function of polymer ratio and (b) metal nanocomposite polysulfone membranes
- Figure 18: Concentration dependent response of 50:50 hydrogel in the presence of (a) alginic acid and (b) tannic acid.
- Figure 19 (a) Calibration curves of PSF-PVA hydrogel in the presence of (a) alginic acid, (b) tannic acid
- Figure 20: Concentration dependant SWV of PSF/Ni in the presence of tannic acid, (a) oxidation SWV and (b) reduction SWV
- Figure 21: (a) Calibration Curves for (b) Pt/PSF/Co (c) Pt/PSF/Ni in the presence of tannic acid
- Figure 22: (a) Calibration Curves for (b) Pt/PSF/Co (c) Pt/PSF/Ni in the presence of alginic acid
- Figure 23: PSF/Ni in the presence of (a) tannic acid and (b) alginic acid
- Figure 24: Calibration curves of polysulfone nano composite in (a) alginic acid and (b) tannic acid
- Figure 25: Calibration curves PSF-hydrogel in tannic acid
- Figure 26: Calibration curves PSF-hydrogel in alginic acid
- Figure 27: (a) hydrophobic membrane interface (b) hydrophylic membrane interface
- Figure 28: Fixed frequency EIS for PSF/Ni in the presence of (a) alginic acid and (b) tannic acid
- Figure 29: Fixed frequency Impedance of microbial sludge (SAB)
- Figure A1: Wetting experiments for commercial and novel polysulfone composite films

## LIST OF TABLES

Table 1: Lattice parameters of nanoparticle unit cells

Table 2: UV/vis analysis of hydrogel solutions

Table 3: Analytical response of polysulfone hydrogels in the presence of tannic and alginic acid.

Table 4: Comparison of PSF, and PSF modified with nanoparticles in the presence of tannic and alginic acid

Table 5: Polysulfone thin films prepared in the presence of tannic acid and alginic

Table A1: Diffusion coefficients calculated for polysulfones in  $\text{H}_2\text{SO}_4$  and PBS and using  $\text{K}_3\text{Fe}(\text{CN})_6$  as redox probe.

Table A2: Diffusion coefficients calculated under hydrodynamic conditions for polysulfones in  $\text{H}_2\text{SO}_4$  and PBS and using  $\text{K}_3\text{Fe}(\text{CN})_6$  as redox probe.

Table A3: Contact angle measurements of metal nanoparticle modified PSF thin films.

Table A4: Comparison of PSF, PVA and PSF hydrogels electrochemistry in HCl.

Table A5: Comparison of surface analysis with diffusion coefficient.

Table A6: Analytical performance of hydrogels in the presence of alginic acid.

Table A7: Analytical performance of hydrogels in the presence of tannic acid.

Table A8: Analytical performance of hydrogels in under hydrodynamic conditions.

## LIST OF ABBREVIATIONS

AA	:	Alginic acid
AFM	:	Atomic force microscopy
CA	:	Cellulose acetate
CV	:	Cyclic voltammetry
De	:	diffusion coefficient
DMAc	:	N,N dimethyl acetamide
EDS	:	Energy dispersive spectroscopy
EIS	:	Electrochemical impedance spectroscopy
E <sup>0</sup>	:	formal potential
Fcc	:	face center cubic
FTIR	:	Fourier transformer infrared
GA	:	Glutaraldehyde
HCl	:	Hydrochloric acid
Hcp	:	Hexagonal centre cubic
KBr	:	Potassium bromide
MBR	:	membrane bioreactor
NOM	;	Natural organic acid
PES	:	Polyethersulfone
PSF	:	Polysulfone
Pt	:	Platinum electrode
PVA	:	Polyvinyl alcohol
Ra	:	Area roughness
rpm	:	revolution per minute
Sa	:	Surface roughness
SEM	:	Scanning electron microscopy
SPCE	:	Screen printed carbon electrode
SWV	:	Square wave voltammetry
TA	:	Tannic acid
UV	:	Ultra violet visible
$\lambda$	:	wavelength



# 1 INTRODUCTION

## 1.1 Hydrophobicity vs hydrophilicity of membranes:

Hydrophilicity can be characterized in general terms as the affinity of the membrane material for water or ability of the membrane to become wetted with water. It has generally been agreed that the increase of membrane hydrophilicity could reduce its fouling (Li et al. 2006). Hydrophobic interaction between solutes or microbial cells and membrane material is regarded as one of the predominant fouling mechanisms. Therefore membrane fouling is expected to be more severe for hydrophobic than hydrophilic membranes (Yu et al. 2005, Sun et al. 2006).

Hydrophilic (water loving) compounds have an affinity to water and are typically charged or have polar side groups to their structure which allows them to attract water. Hydrophobic (water hating) compounds are repelled by water and are typically neutral (no charge.) Hydrogen bonds are very strong bonds that exist between water molecules. Therefore water molecules are highly attracted to each other and excludes (repels) the hydrophobic molecules

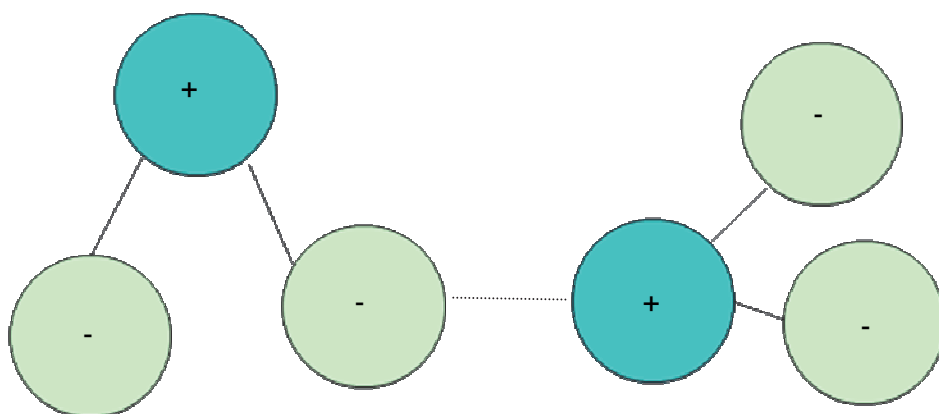


**Figure 1:** Structure of water showing charge interactions between water molecules

Therefore a hydrophilic membrane will not be fouled with oil, grease or other hydrophobic substances. The membrane is highly attractive to water so the water molecules will push away other molecules in order to gain access to the membrane

In Physical Chemistry molecular interactions may be defined as follows;

- (i) the generation of random paired charges throughout the molecule (Londons dispersion forces) typically interaction between hydrocarbons;
- (ii) interaction between permanent or induced dipoles called polar interactions;
- (iii) interaction between permanent charges which are called ionic interactions.

However in Biochemistry and Biology bio-molecules are understood to be large and may contain many types of interactive groups. Therefore, if the overall property of the molecule was hydrocarbon-like and interacted predominantly with other molecules dispersively the molecule was designated as hydrophobic, since hydrocarbons and water were immiscible. Alternatively, if polar groups dominated in the macromolecule the molecule was said to be hydrophilic.

There has been much research into the hydrophilization of ultrafiltration membrane materials. This research includes blending of a hydrophilic polymer or metal nanoparticles,

with the membrane-forming polymer to obtain hydrophilic membranes. Hydrophilic polymer additives include polyvinylpyrrolidone (PVP) and polyethylene glycol (PEG) (Hashim, Liu & Li 2009, Ju et al. 2009, Sagle et al. 2009). Despite its importance, only few studies focused on the influence of different polymeric membrane materials on membrane fouling in MBRs. It has been reported that hydrophilic cellulosic membrane are more successful with respect to fouling than hydrophobic polysulfone membranes (Howell, Sanchez & Field 1993). However, some researchers have reported that the hydrophobic membranes have a relatively low fouling tendency with less adsorption onto the surface than hydrophilic counterparts (Nomura, Fujii & Suzuki 1997).

Choo and Lee investigated the novel approach to better understand fouling in terms of surface energy charges involved. They tested three different types of membrane materials i.e. cellulose, polysulfone and fluoropolymers and found the most hydrophobic fluoropolymer to show the lowest fouling tendency (Choo, Lee 2000). A commonly known fluoropolymer is Teflon. It has also been shown that further changes in membrane hydrophobicity occur with other membrane modifications such as pore size and morphology. This fact makes the correlation between membrane hydrophobicity and fouling more difficult to assess (Maximous, Nakhla & Wan 2009). In fact, Maximous et al. concluded in 2009 that in the case of sludge filtration for hydrophilic and hydrophobic membranes, hydrophilicity does not seem advantageous from the fouling propensity. Hydrophilic membranes do however have higher cake resistance reversibility than hydrophobic membranes.

When comparing polymer membranes with hydrophilic properties, cellulose membranes shows remarkable hydrophilic property due to three active hydroxyls in each repeating unit of cellulose molecule (Li et al. 2006).

The strong hydrogen bonds that occur between cellulose chains prevents that the material dissolve in ordinary solvents and it can withstand very high temperatures. Cellulose acetate and regenerated cellulose membranes have been widely applied in technologies such as ultrafiltration, microfiltration and dialysis. However, cellulose is degraded during the regeneration process and this causes irreversible damage to its ability of enduring strong acid, alkali and organic solvents, as well as serious environmental problems.

Because of its robustness and its ability to withstand strong acids and alkalis, polysulfone and polyethersulfone still remain a more practical choice for membrane filtration than the more hydrophilic cellulose.

## **1.2 Metal nanoparticle modified membranes**

Many studies have been conducted to increase the hydrophilic properties of the polysulfone membrane surface. These studies can be divided into three categories: 1) blending PSF with hydrophilic nanoparticles such as  $\text{SiO}_2$ ,  $\text{ZrO}_2$  and  $\text{TiO}_2$ , 2) grafting with hydrophilic polymers, monomers or functional groups and 3) coating with hydrophilic polymers (Yanan et al. 2007). Of the aforementioned methods, blending with nanoparticles has attracted much interest in the past 10 years due to their convenient operation and mild conditions. Blending offers the advantage for the preparation of artificial membranes with excellent separation performance, good thermal and chemical resistance and adaptability to the harsh wastewater environments (Maximous et al. 2009).

Blending involves firstly dissolving/dispersing the metal nanoparticles in solvent, which in the case of polysulfone is either *N,N'*-dimethylacetamide (DMAc) or *N*-methyl-2-pyrrolidone (NMP). This solution is then sonicated for 72hr at approximately 60°C to obtain a uniform and homogeneous casting suspension. The polymer solution is then added to the solution and the mixture is then further sonicated for 1 week until a homogeneous solution is formed. Membranes are then cast onto a glass plate using the phase inversion method.

Phase inversion is a process whereby a polymer is transformed in a controlled manner from a liquid to a solid state. The process of solidification is often initiated by the transition from one liquid state into two liquids (liquid-liquid demixing). At a certain stage during demixing, one of the liquid phases (the high polymer concentration phase) will solidify so that a solid matrix is formed. By controlling the initial stage of phase inversion the membrane morphology can be controlled i.e. porous as well as non-porous membranes can be prepared. The concept of phase inversion covers a range of different techniques such as solvent evaporation, thermal precipitation and immersion precipitation.

Most commercially available membranes are prepared using immersion precipitation. A solution of polymer and solvent is cast on a suitable support and immersed in a coagulation bath containing a nonsolvent. Precipitation occurs because of the exchange of solvent and nonsolvent and eventually the polymer precipitates. Water is most often used as nonsolvent, but organic solvents such as methanol can be used as well. The membrane structure ultimately obtained, results from a combination of mass transfer and phase separation. Other preparation parameters to consider are: evaporation time, polymer concentration, humidity, temperature and composition of casting solution. These parameters mainly determine the ultimate membrane performance.

In recent years, various metal nanoparticles have been used in wastewater treatment membrane technology with varied success. Previous studies have investigated the effectiveness of  $\text{TiO}_2$ ,  $\text{Al}_2\text{O}_3$ , Ag,  $\text{Fe}_3\text{O}_4$  and most recently  $\text{ZrO}_2$  nanoparticles as membrane filler for the treatment of wastewater (Zodrow et al. 2009).

Nanocomposite membranes can remediate two types of fouling: membrane fouling due to organic matter and biofouling. Titania nanoparticles have mostly been used to mitigate the former. Li et al. showed that water flux through a polyethersulfone- $\text{TiO}_2$  membrane was significantly enhanced, but the effect was concentration dependent. This is due to nanoparticle agglomeration (Kim, Van der Bruggen 2010). Other studies have however contradicted this finding (Yanan et al. 2007) and it must therefore be noted that different findings may arise from differences in procedures and materials.

Titanium dioxide ( $\text{TiO}_2$ ) nanoparticles have emerged as a promising photocatalyst for water and wastewater purification.  $\text{TiO}_2$  nanoparticles are very versatile and can serve both as oxidative and reductive catalysts for organic and inorganic pollutants.  $\text{TiO}_2$  has been proven effective in degrading organic compounds and reducing toxic metal ions under UV light. Nano- $\text{TiO}_2$  as an active nano-material has many advantages such as UV-resistance, super hydrophilicity and innocuity. Therefore it is currently being applied to a variety of problems that are of environmental interest, in addition to water and air purification (Yanan et al. 2007).

Biofouling is avoided by using the bactericidal properties of nanoparticles. Silver is the most commonly used bactericide used for fouling reduction. Silver impregnated membranes have been proven to be effective against two strains of bacteria, *E. coli* K12 and *P. mendocina* KR1 that are both found in wastewater (Omidian, Rocca & Park 2005). These membranes are not only antimicrobial, but they also prevent bacterial attachment to the membrane surface and thus reduce biofilm formation. Additionally, silver nanocomposite PSF membranes showed a significant improvement in virus removal from wastewater.

The most recent metal nanoparticle composite membranes that have been investigated for wastewater filtration are  $\text{Al}_2\text{O}_3$ /polyethersulfone (PES) and  $\text{ZrO}_2$ /PES membranes (Maximous et al. 2009). Maximous identified polymer concentration as the most important parameter for tailoring membrane properties. He found that with an increase in polymer concentration from 10%-18%, the deionised water permeation decreased from 1227.4  $\text{L/m}^2\text{bar-h}$  to 866.5  $\text{L/m}^2\text{bar-h}$  suggesting that increased polymer concentration forms a thicker and denser skin layer. The steady state fouling rate of  $\text{Al}_2\text{O}_3$ /polyethersulfone ( $1.25 \times 10^{-11} \text{ L/m}^2\text{bar-h}$ ) membranes was also found to be significantly lower than the unmodified PES membrane ( $0.005 \text{ L/m}^2\text{bar-h}$ ). This is ascribed to the reduced hydrophobic adsorption between sludge particle and the  $\text{Al}_2\text{O}_3$ /polyethersulfone (PES) membrane.

Maximous et al. extended this research to zirconia ( $\text{ZrO}_2$ ), as zirconia membranes are known to be chemically more stable than titania and alumina membranes and therefore are more suitable for liquid phase applications under harsh conditions. The addition of  $\text{ZrO}_2$  nanoparticles to the PES casting solution enhances the membrane strength, but slightly affects the membrane thickness. The zirconia entrapped membrane also showed lower flux decline, improved total and cake resistance and fouling resistance compared to the unmodified membrane. The steady state fouling rate decreased from 0.005 to  $1.04 \times 10^{-5} \text{ L/m}^2\text{bar-h}$ . Chen et al. prepared embedded nano-iron polysulfone membranes for dehydration of ethanol/water mixtures by pervaporation (Chen et al. 2008). It was found that the embedded nanoparticle slightly increased the flux and also increased the membrane separation factor. The nano-iron composite membrane also showed an obvious effect on the permeation and sorption behaviours of embedding membranes. This study proposed that nano iron affected the ordering/packing of the polymer chains and some of the particle oxide, which influenced the hydrophilicity.

Nano composite membranes can remediate two types of fouling: membrane fouling due to organic matter and bio fouling. Titania nanoparticles have mostly been used to mitigate the former. Li et al. showed that water flux through a polyethersulfone- $\text{TiO}_2$  membrane was significantly enhanced, but the effect was concentration dependent. This is due to nanoparticle agglomeration (Kim, Van der Bruggen 2010). Other studies have however contradicted this finding (Yanan et al. 2007) and it must therefore be noted that different findings may arise from differences in procedures and materials. Titanium dioxide ( $\text{TiO}_2$ ) nanoparticles have emerged as a promising photocatalyst for water and wastewater purification.  $\text{TiO}_2$  nanoparticles are very versatile and can serve both as oxidative and reductive catalysts for organic and inorganic pollutants.  $\text{TiO}_2$  has been proven effective in degrading organic compounds and reducing toxic metal ions under UV light. Nano-  $\text{TiO}_2$  as an active nano-material has many advantages such as UV-resistance, super hydrophilicity and innocuity. Therefore it is currently being applied to a variety of problems that are of environmental interest, in addition to water and air purification (Yanan et al. 2007).

Biofouling is avoided by using the bactericidal properties of nanoparticles. Silver is the most commonly used bactericide used for fouling reduction. Silver impregnated membranes have been proven to be effective against two strains of bacteria, *E. coli* K12 and *P. mendocina* KR1 that are both found in wastewater (Omidian, Rocca & Park 2005). These membranes are not only antimicrobial, but they also prevent bacterial attachment to the membrane surface and thus reduce biofilm formation. Additionally, silver nano composite PSF membranes showed a significant improvement in virus removal from wastewater.

The most recent metal nanoparticle composite membranes that have been investigated for wastewater filtration are Al<sub>2</sub>O<sub>3</sub>/polyethersulfone (PES) and ZrO<sub>2</sub>/PES membranes (Maximous et al. 2009). Maximous identified polymer concentration as the most important parameter for tailoring membrane properties. He found that with an increase in polymer concentration from 10%-18%, the deionised water permeation decreased from 1227.4 L/m<sup>2</sup>bar-h to 866.5 L/m<sup>2</sup>bar-h suggesting that increased polymer concentration forms a thicker and denser skin layer. The steady state fouling rate of Al<sub>2</sub>O<sub>3</sub>/polyethersulfone (1.25 E-11 L/m<sup>2</sup>bar-h) membranes was also found to be significantly lower than the unmodified PES membrane (0.005 L/m<sup>2</sup>bar-h). This is ascribed to the reduced hydrophobic adsorption between sludge particle and the Al<sub>2</sub>O<sub>3</sub>/polyethersulfone (PES) membrane.

Maximous et al. extended this research to zirconia (ZrO<sub>2</sub>), as zirconia membranes are known to be chemically more stable than titania and alumina membranes and therefore are more suitable for liquid phase applications under harsh conditions. The addition of ZrO<sub>2</sub> nanoparticles to the PES casting solution enhances the membrane strength, but slightly affects the membrane thickness. The zirconia entrapped membrane also showed lower flux decline, improved total and cake resistance and fouling resistance compared to the unmodified membrane. The steady state fouling rate decreased from 0.005 to 1.04E-05 L/m<sup>2</sup>bar-h.

Chen et al. (2008) prepared embedded nano-iron polysulfone membranes for dehydration of ethanol/water mixtures by pervaporation (Chen et al. 2008). It was found that the embedded nanoparticle slightly increased the flux and also increased the membrane separation factor. The nano-iron composite membrane also showed an obvious effect on the permeation and sorption behaviours of embedding membranes. This study proposed that nano iron affected the ordering/packing of the polymer chains and some of the particle oxide, which influenced the hydrophilicity.

### 1.3 Hydrogels

Hydrogels are hydrophilic polymer chain networks, capable of absorbing water up to 99.9 % owing to its high absorbent nature. They conjointly possess a degree of flexibility, owing to their vital water content. They may also be described as three-dimensional network structures obtained from a category of artificial or natural polymer that retain a vital quantity of water (Syed et al. 2011). They are present as considerably dilute cross-linked systems that are classified as weak or strong depending on their flow behaviour under steady state conditions. However, traditional hydrogels exhibit very little flow under steady state conditions and has the form of a solid jelly like material with properties similar to the starting material; ranging from soft and weak to mechanically stable and rough. Introducing a crosslinking agent into the polymer network improves the flow behaviour and contributes to the stickiness of hydrogels. Several investigators have developed polysulfone membranes,

targeted on improving polysulfone's hydrophobic nature using different approaches and for different applications (Susanto, H et.al; 2008). Hydrophilic polysulfone membranes are appropriate for use in applications requiring low macromolecule binding and high separation efficiency. The hydrophilic polysulfone membranes are beneficial for a large variety of filtration applications (Fan et al. 2008).

Hydrophilic polysulfone may be achieved by incorporating a hydrophilic polymer into the polysulfone network such as polyvinyl alcohol. The hydrophilic functional groups like radical (OH) or carboxyl (COOH) and their characteristic chains are responsible for water storage and water absorption (Schacht E.H. et.al; 2008). Hydrogels find application in different areas of separation chemistry such as metallurgy, petrochemical, food industries, medicine (drug delivery and blood purification), electronics (electrical devices) and environmental remediation (water treatment).

Conducting polymers are a new class of polymers with unique chemical and electrochemical properties. Introducing a conducting polymer such as polyaniline into the polysulfone membrane will enhance the permeability and reduce the fouling of the membrane (Owino et al. 2008). Polyaniline nanoparticles inclusion within the polysulfone membrane improved water flux and salt rejection and not only increase the separation characteristics, but also altered the membrane morphology and surface roughness. The contact angle decreased with an increase in polyaniline and cobalt nano composite (Fan et al. 2008). Polyaniline nanoparticles inclusion within the polysulfone membrane improved water flux and salt rejection and not only increase the separation characteristics, but also altered the membrane morphology and surface roughness

Polyvinyl alcohol (PVA) is soluble polymer with extremely hydrophilic properties, physical and chemical stability, PVA is a type of excellent membrane material for preparation of a hydrophilic membrane. Specifically, PVA-polyvinyl acetate, PVA-vinyl compound, PVA-vinyl resin, these polymer are more desirable for the preparation of hydrophilic membranes due to its low cost, business convenience, high water porosity and smart film-forming properties. Many PVA membranes have been developed for reverse osmosis and most of those membranes provide comparatively low flux and low salt rejection. Abdel-hameed and El-Aassar 2012 [15] confirmed that membrane preparation of polysulfone modified with PVA and TiO<sub>2</sub> at 75°C for a time frame of 60 minutes gave an optimum reverse osmosis membrane performance for neat PSF/PVA/TiO<sub>2</sub> with permeate flux starting from 9.32 L/m<sup>2</sup>h to 11.56 L/m<sup>2</sup>h with a slight increase in salt rejection from 76.79 to 78% therefore they reported salt rejection improved as a function of cross linker concentration.

In most cases literature reports on metal nanoparticle oxides and or conductive polymers in conjunction with metal nanoparticle oxides. In this work we have endeavoured to produce hydrophilic polysulfone membranes using simplified chemical strategies to produce stable and reproducible hydrophilic polysulfone derivatives. The research approach is based on a primarily academic consideration of the chemical and physical properties that render a membrane hydrophilic. Therefore it was also necessary to compare the synthesised polysulfone composites in some way to existing commercial membranes. It was also necessary to identify model compounds for the quantitative evaluation of polysulfone composite analytical performance.

Natural organic matter (NOM) is known to be the worst foulant in the membrane processes, but the complexities of NOM make it difficult to determine its effects on membrane fouling. Therefore, simple organic compounds (surrogates for NOM) are used in research to investigate the fouling mechanisms in ultrafiltration. Previous research on NOM components in membrane processes indicated that polysaccharides formed an important part of the fouling cake. From literature the NOM components are made up of polysaccharides (e.g. dextran, alginic acid, and polygalacturonic acid) and small carbohydrates (e.g. tannic acid) were evaluated for their removal in softening (the treatment process in the City of Austin). (Kweon et al. 2005) For the purpose of quantitative evaluation of membrane transport properties and analytical performance by electrochemical methods, we have selected alginic acid and tannic acid as target molecules.

## **OBJECTIVES AND AIMS**

### **Objective 1: Evaluation of the status quo of polysulfone modification by metal nanoparticle incorporation**

#### **AIM 1**

Comprehensive literature review on metal nanoparticle modified polysulfone membranes and its application in water treatment, with careful attention to the modifications effected to improve fouling properties of the modified membrane systems.

### **Objective 2: Synthesis and characterisation of novel polysulfone composites with reduced hydrophobicity**

#### **AIM 2**

Synthesis of polysulphone thin films modified with Co and Ni nanoparticles by chemical and electrochemical methods from readily available laboratory reagents and optimising synthesis conditions. The chemically synthesised polysulphone (PSF) material will be evaluated in terms of processability of the material and fundamental electrochemistry.

#### **AIM 3**

Modification of the PSF membrane by chemical crosslinking to produce polysulfone hydrogels, followed by spectroscopic and morphological characterisation of the modified PSF materials will be done. The effect of PSF contribution on hydrophilicity and morphology will be evaluated.

### **Objective 3: Analytical response of polysulfone nanocomposites using model organic compounds in laboratory scale experiments.**

#### **AIM 4**

The analytical response of polysulfone composites and hydrogels will be evaluated as concentration dependent chemical sensor response in the presence of model organic compounds. The fouling ability will be assessed in terms of sensitivity of the membranes to individual compounds and the time to passivation of the membrane material.

## **2 EXPERIMENTAL**

The metal nanoparticles, modified polysulfone and polysulfone hydrogel materials were all prepared in house from commercially available laboratory reagents under standard laboratory conditions. The polysulfone materials were characterised using spectroscopy,

electron microscopy, drop shape analysis and electrochemistry tools available in our laboratories.

### **(i) Metal nanoparticle modified polysulfone nano composite**

#### *Preparation of PSF films*

PSF films were prepared by dissolving polysulphone in N,N-dimethyl acetamide to give a final concentration of 0.08 g.ml<sup>-1</sup>, followed by dropping small volumes (2  $\mu$ l aliquot) of the solution onto the Pt electrode with a micropipette. For freestanding films, solutions were cast in glass beaker by swirling beaker with H<sub>2</sub>SO<sub>4</sub> and polysulphone solution to obtain a homogenous film. Films were rinsed thoroughly with deionised water and allowed to dry for at least 24hrs. The metal nanoparticle modified thin films were produced by adding the desired amount of metal nanoparticle/ethanol solution to the dissolved polysulfone solution. Thin films or freestanding films were prepared as before.

#### *Synthesis of Co nanoparticles*

Cobalt salt (CoCl<sub>2</sub>.6H<sub>2</sub>O) was dissolved in ethanol to form a dark blue solution. A mixture of hydrazine hydrate (N<sub>2</sub>H<sub>4</sub>.H<sub>2</sub>O) and sodium hydroxide (NaOH) was added to the dark blue solution at room temperature. After about 30s gray solid particles formed. These were precipitated by placing a magnet under the container. The particles were washed completely with distilled water, ethanol and absolute ethanol and stored in absolute ethanol.

#### *Synthesis of Ni nanoparticles*

Nickel chloride hexahydrate was dissolved into absolute ethanol to form solution a, ([Ni<sup>2+</sup>] = 0.333M). For solution b, potassium hydroxide and hydrazine hydrate was mixed together. Solution a was poured into solution b with immediate vigorous magnetic stirring at room temperature. The overall reaction time was 2 hrs. The resultant product was washed thoroughly with deionised water and then with acetone. The final black particles were stored in ethanol in a closed bottle.

### **(ii) Hydrogel synthesis**

PSF-PVA hydrogels was synthesised by dissolving 0.4421g of polysulfone crystal into 50 mL of N,N-dimethylacetamide (DMAc) to produce 0.0554 M PSF-solution after 1 hour of sonication. 5 mL of this solution was transferred to a round bottom flask, to which 2.5895g of PVA was added. To the mixture 1 mL glutaraldehyde cross-linker solution was added followed by the catalyst in order to speed up the reaction during the crosslinking process. An excess of acid was required for protonation and reduction of the aldehyde into alcohol. 1 mL of 2 M HCl catalyst was added the reflux mixture and the mixture was allowed to for 3 hours at 75°C with constant stirring. After three hours the mixture was stored at a room temperature for 10 days in order to ensure completeness of cross-linking reaction. The cross linking of PVA and PSF was controlled at three different ratios to evaluate the effect of the PSF contribution i.e. 25:75, 50:50 and 75:25.

## **3 EXPERIMENTAL PROCEDURES**

Spectroscopy refers to the measurement of radiation intensity as a function of wavelength, and is typically used for qualitative and qualitative analysis of materials. FTIR spectroscopy was performed on drop coated thin films of the polysulfone metal nanoparticle composites,



PVA, gluteraldehyde, PSF an hydrogels, for confirmation of surface composition. Scanning electron microscopy (SEM) is used for the study of surface morphology, topography, composition of a material. A conductive sample is scanned with a high-energy beam of electrons in raster scan pattern and the resulting secondary back scattered electrons are measured. SEM and HRTEM were performed on the metal nanoparticles in order to determine their shape and size. SEM with EDAX was performed on polysulfone nanoparticle composites and hydrogels to determine elemental composition. In atomic force microscopy (AFM) the force between a probe and the sample is measured as the angle of deflection between the sample and cantilever probe. It does not only measure the force acting on the material but also regulates it, and acquisition of images is achieved at very small forces. AFM was used to study the surface morphology of PSF. PSF/Ni, PSF/Co and hydrogels as thin films onto microscope slides. Drop shape analysis of pure water on PSF. PSF/Ni, PSF/Co and hydrogels as thin films onto microscope slides, was done to measure contact angle.

Electrochemistry provides information of the material being analysed from the current response and peak potential response. The signal produced will enable the calculation of a diffusion constant which may be related to the rate at which electrons move to and into the interfacial region of the transducer. Cyclic voltammetry is a widely used electro analytical technique for the evaluation of redox properties of conductive and semi-conductive materials. The materials under investigation are usually immobilised at a transducer surface, which may be macro-electrodes, predominantly micro-electrodes and even screen printed or inter-digitated electrodes. The latter providing working, counter and reference electrodes in a neat compact arrangement, for application in small volume electrochemical cells. A potentiostat is used to produce the input signal and the resultant output of current against potential is presented as a voltammogram. The forward scan produces a current peak for any analyte that can be reduced or oxidized depending on the initial scan direction over the range of potential scanned. The current increases as it reaches the reduction potential of the analyte, but then decreases as the concentration of the analyte is depleted close to the electrode surface. If the redox couple is reversible, then reversing the applied potential makes it reach a potential that re-oxidizes the product formed in the first reduction reaction, thus producing a current of reverse polarity from the forward scan. The oxidation peak usually has the same shape as that of the reduction peak. As a result, the information about the redox potential and the electrochemical reaction rates of compounds can be obtained. For instance, if the electron transfer is fast at the electrode surface and the current is limited by the diffusion of species to the electrode surface, then the peak current is proportional to the square root of the scan rate ( $v^{1/2}$ ). Square wave voltammetry is a variation of cyclic voltammetry where the forward and reverse scans are separated and a square wave form is imposed on the applied potential to remove the capacitive current and report only Faradaic current related to redox processes. In this way a more sensitive current voltage response is obtained.

## **METHODOLOGY**

The polymer composites and hydrogel networks synthesised in this work was characterised by spectroscopic, morphological, electron microscopic, drop shape analysis as well as electrochemical methods.

Spectroscopy is the study of the interaction between matter and radiated energy. Spectroscopy is the measurement of radiation intensity as a function of wavelength, used for qualitative and quantitative analysis methods and even quantum physics. Molecules have distinctive spectra, which provide qualitative and quantitative information regarding the vibrations of bonds between atoms and molecules. FTIR spectroscopy was used to evaluate the cross linking of polymers to produce the hydrogel. Characteristic stretching vibrations for the starting materials and final products were compared to establish a mechanism for the formation of the final product.

Scanning probe microscopy (SPM) describes a broad group of instruments used to image and measure properties of material, chemical and biological surfaces. The SPM images are obtained by scanning a sharp probe across the surface while examining and collecting the tip sample interactions to produce an image. Atomic force microscopy (AFM) functions by measuring force between a probe and the sample. AFM measures the vertical and lateral deflections of the cantilever. In non-contact mode at tip-sample separations of 10 to 100nm is operated, forces such as van der Waals, electrostatic, magnetic forces can be sensed and give information about surface topography, distribution of charges. In contact mode, the tip is in contact with the sample surface through any adsorbed gas layer, the tip scans across the sample under action of a piezoelectric actuator, either by moving the sample or the tip relative to the other. Information about the surface morphology and roughness was related to the hydrophobicity of the polymer composites and hydrogels.

The scanning electron microscope (SEM) is widely use as research technique in membrane technology for identification of surface morphology, porosity and pore sized distribution of a material. A centred beam of high-energy electrons is used to generate secondary electrons that will interact with the surface of solid specimens. The signals derived from electron-sample interactions reveal information regarding the sample morphology, chemical composition, crystalline structure and orientation of materials. SEM was used to evaluate the size and shape of nanoparticles synthesised (in house) by chemical methods. SEM was also used to evaluate the pore size and shape distribution in polysulfone metal nanoparticle composites. The effect of polymer concentration and effectiveness of crosslinking was also evaluated using SEM.

Contact angle is a quantitative measure of the wettability of a solid by a liquid. The deliquescent and hydrophobic properties are predicted by the contact angle being measured. If the water contact angle is smaller than 90°C it is indication of hydrophilic and if it water contact angle is larger than 90°C it is indication of hydrophobic nature of the material. Contact angle was used as the physical method for quantifying the improved hydrophilic nature of hydrogels synthesised.

Electrochemical methods may be divided into AC and DC voltammetric applications. DC voltammetry includes methods such as cyclic, square wave and differential pulse voltammetry. In each of these methods a classical three electrode system is employed with the working electrode functionalised with the polymer composite or hydrogel of choice. A perturbing signal (current or voltage) is applied to the working electrode and the response (voltage or current) is measured displayed as a current-voltage curve. These voltammograms may be qualitatively and quantitatively evaluated to derive information about the redox chemistry and interfacial kinetic parameters associated with a particular solution

interface. Qualitative evaluation of the polymer composites and hydrogels as thin films at the working electrode interface was related to the energy requirements for material performance whereas quantitative information relating to analytical performance was extracted using suitable graphs and equations. AC voltammetry involves sinusoidal stimulation of the input signal that facilitates probing of the interface and bulk material of thin film materials at the working electrode. The data produced are also sinusoidal and requires equivalent circuit modelling to extract information about capacitance and charge transfer resistance changes at the solution interface. The AC technique, electrochemical impedance spectroscopy, was used to evaluate the diffusion and analytical performance of the polymer composites and hydrogels in the presence of the model compounds, as a means to assess fouling behaviour.

### **Experimental details:**

High resolution SEM and TEM of Co and Ni nanoparticles, thin films of PSF, PSF/Co and PSF/Ni and polysulfone hydrogels prepared by drop coating were analysed on Zeiss instrument available at Physics department (UWC). Raman spectroscopy of drop coated thin films onto microscope slides were analysed on Horiba Jobin ExploRa Raman instrument and AFM analysis was performed on Nanosurf AFM (Wirsam). FTIR analysis was performed on Bruker instrument on solution and thin films where applicable.

Cyclic voltammetry, square wave voltammetry were performed using a three electrode cell with the polysulfone materials drop coated as thin films onto the working electrode. The counter electrode was a thin platinum wire and the reference electrode was Ag/AgCl (BAS microelectrodes). Electrochemical impedance analysis was performed on Voltalab and Zahner instruments using the same three electrode cell as for voltammetry. Contact angle measurement was performed on a Kruss drop shape analyser. All chemicals and electrodes were supplied by local suppliers. Ultra high quality water (MilliQ, 18 Ohm; Millipore) was used in the preparation of analytical solutions

## **4 RESULTS AND TREATMENT OF DATA**

### *SEM and HRTEM of Co and Ni nanoparticles:*

Cobalt nanoparticles can form three crystal structures; the face centered cubic (fcc), hexagonally closed packed (hcp) and epsilon [14]. The hcp structure is stable at low temperatures and the fcc stable at higher temperatures above 450° C [14]. HR-TEM confirmed the Cobalt nanoparticles were predominantly present in the hcp-Co formation with long sides in the order of 50 nm (figure 2).

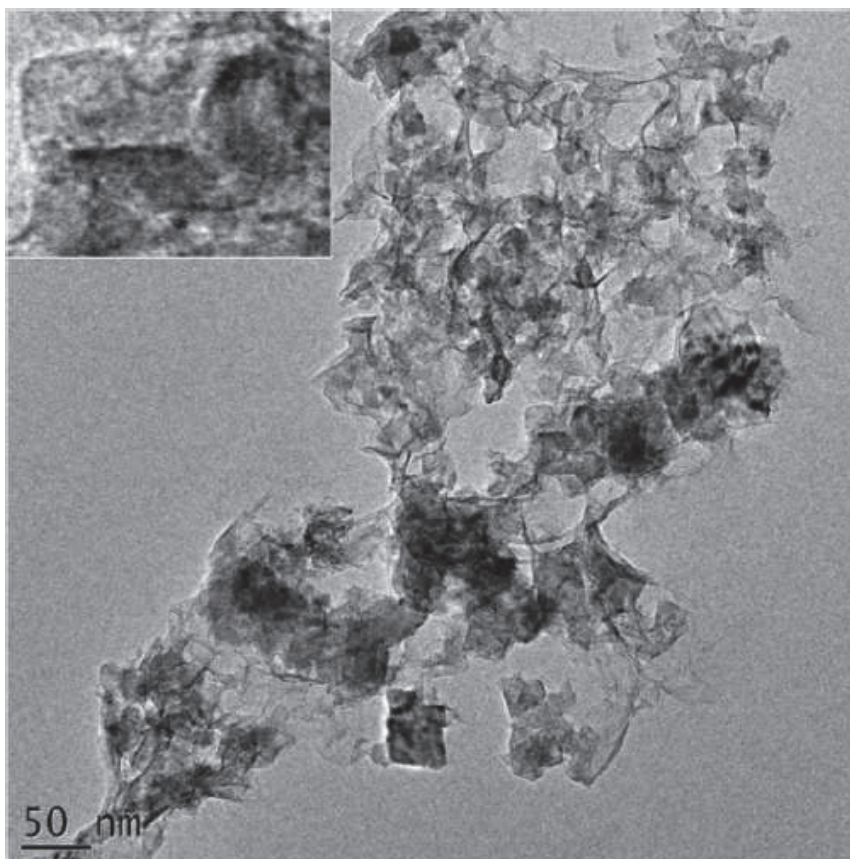


**Figure 2:** HRTEM of Co nanoparticles

The EDAX spectrum confirmed the presence of Co, Cl (from starting material) and Cu (from grid used as support for nanoparticle analysis (figure 3)).

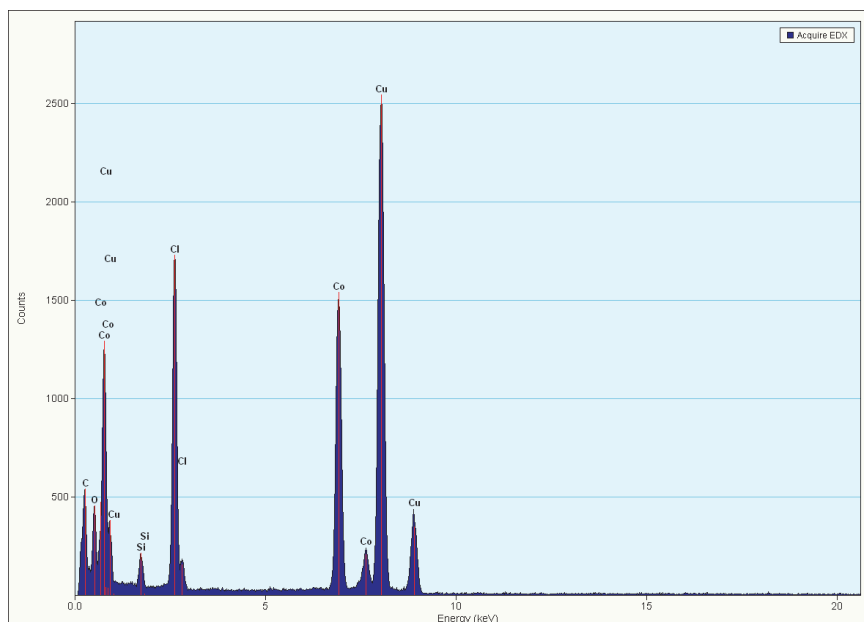


**Figure 3:** EDX spectrum of the Co nanoparticles

The HRTEM image of the Ni nanoparticles confirms a cubic shape, favouring the face centered cubic crystalline form of Ni nanoparticle (figure 4). The dimensions of the cubic

nanoparticles were observed to be approximately 5 nm on either face. The Ni(II) forms complexes with three different geometries i.e. tetrahedral, octahedral and square planar.. Ni nanoparticles are useful in catalysis, conducting inks and magnetic materials.

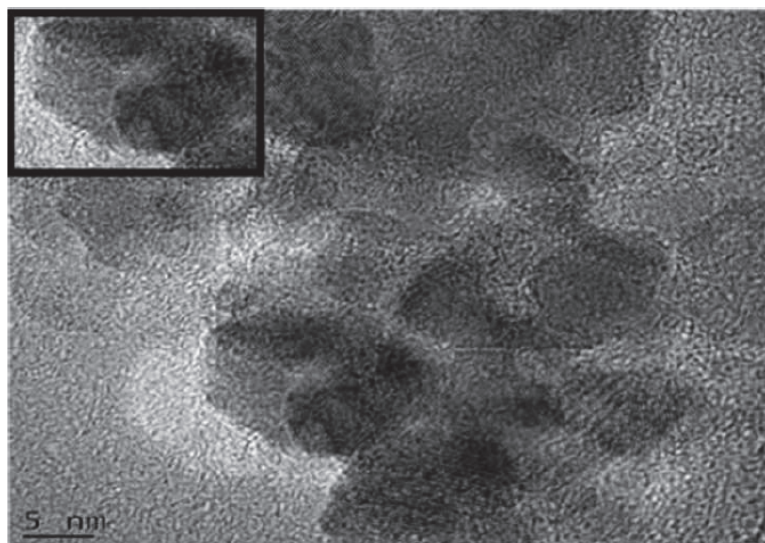


**Figure 4:** HRTEM of Ni nanoparticles

The EDX spectrum of the Ni nanoparticles confirms the presence of nickel nanoparticles, with energy lines in the region of 8-9 keV which are the K lines and also in the region of 0.8-1 keV which are the L lines

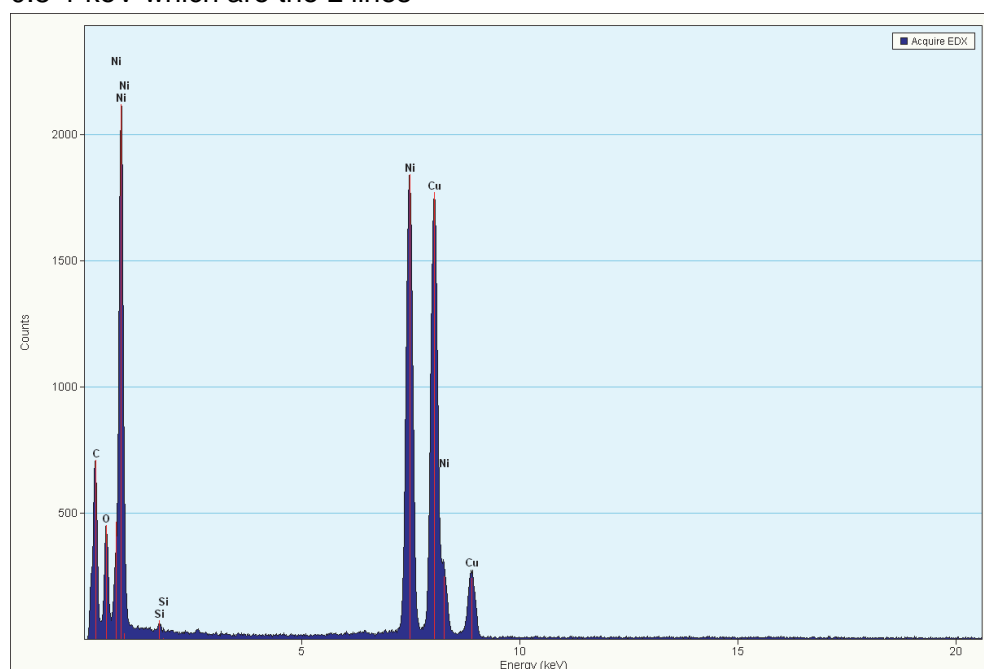


**Figure 5:** EDX spectrum of the Ni nanoparticles

Crystal lattice is a systematic arrangement of atoms that are found in crystals with the exception of amorphous solids and gases. A unit cell is the smallest component of the crystal lattice and illustrates the arrangement of atoms in a crystal. The unit cell is characterized by its lattice parameters which consist of the length of the cell edges and the angles between them. The lattice constant and also known as lattice parameter refers to the

constant distance between unit cells in a crystal lattice. The lattices in three dimensions generally have three lattice constants: a, b, and c. In case of cubic crystal structures, all of the constants are equal and referred only as a. However, in case of hexagonal crystal structures, the a and b constants are equal, and only referred to as a and c constants [26]. Ni nanoparticles are known to favour a cubic close packed arrangement (or fcc) whereas Co nanoparticles favour a hexagonal closed packing (hcp) arrangement [11-27]. However the packing efficiency of both these packing arrangements are high (74%) with co-ordination number of 12. In a fcc unit cell the atoms touch along the face diagonals and the lattice parameter may be calculated from equation 1 as follows:

$$4r = a(2)^{1/2} \quad (1)$$

Where r, is the radius of Ni = 0.1246 nm

For the hcp close packing arrangement the lattice parameters a (=b) and c may be calculated from the radius as follows using equations 2 and 3:

$$a = 2r \quad (2)$$

$$\text{and } 2a = [(a / \sqrt{3})^2 + (c/2)^2]^{1/2} \quad (3)$$

where r is the radius of Co = 0.1253 nm

The lattice parameters for Co and Ni nanoparticles were calculated based on unit cell dimensions identified from TEM measurements (Table 1)

**Table 1:** Lattice parameters of nanoparticle unit cells

Metal nanoparticle	Nanoparticle size (nm)	Membrane pore size (μm)	Lattice parameters a,b,c (Å)
Cobalt	h=b=50, l=100	2-8	a=2.506 x 10 <sup>-11</sup> c=8.32 x 10 <sup>-12</sup>
Nickel	l=5	0.5-1.5	2.49 x 10 <sup>-11</sup>

From the data calculated it became clear that the metal nanoparticle size and close packing arrangement directed the shape and size of pore formation. Nickel nanoparticles with the smallest particle size and cubic unit cell produced the smallest pore size in the modified polysulfone membrane, as compared to Co nanoparticles.

From the above table, it is clear that the metal nanoparticle size and close packing arrangement direct the shape and size of pore formation. Nickel nanoparticles with the smallest produced the smallest pore size in the modified polysulfone membrane, followed by Co nanoparticles.

#### **SEM of PSF/Ni and PSF/Co cast films:**

SEM of polysulfone shows a highly branched network structure (figure 5). The elemental analysis spectrum of the unmodified PSF confirms an abundance of sulphur associated with the sulphone groups of the polymer. The SEM image of PSF/Co shows a uniform distribution of pores, with size ranging from 1.75 -7.88 μm. A 3D honey comb structure was observed for PSF/Co and the energy dispersive spectroscopy (EDS) confirmed that the Co nanoparticles were incorporated to the PSF casting suspension as indicated by the spectral band in the range of 6.8 keV to 7.6 keV (figure 7). SEM of PSF/Ni showed very small pores uniformly distributed throughout the cast film. The Ni nanoparticle spectral band was observed in the



range of 7.4 keV to 8.2 keV from EDS measurements (figure 8). SEM of PSF/Ag showed a uniform distribution of pores, with pore sizes ranging from 10.73-15.88  $\mu\text{m}$ .

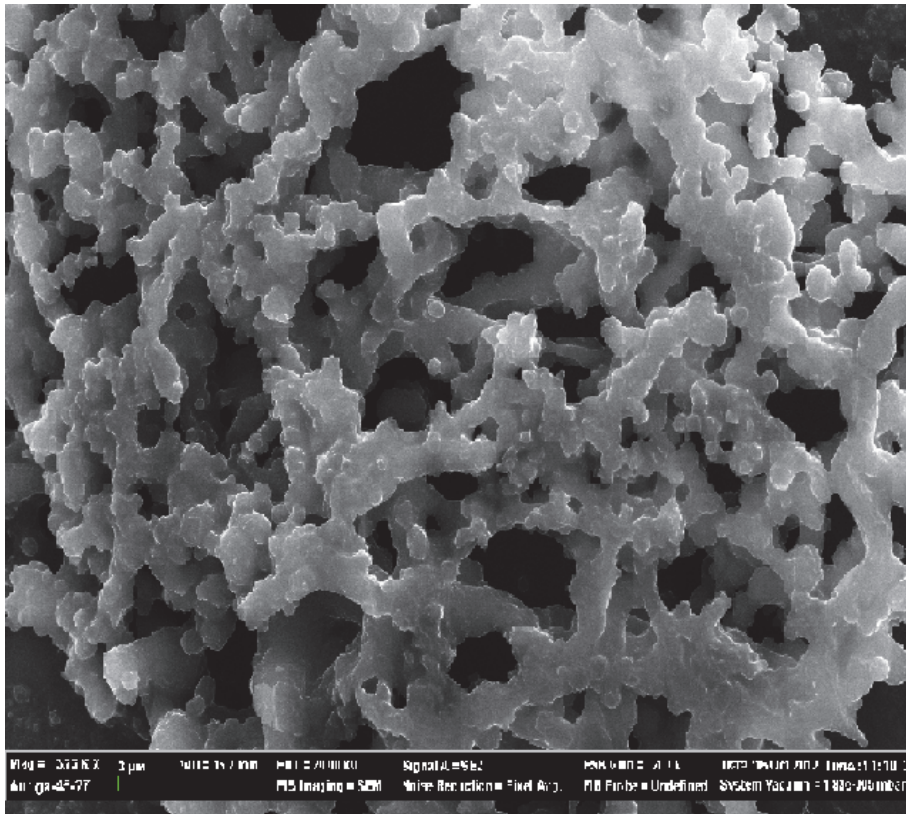


**Figure 6:** SEM of PSF

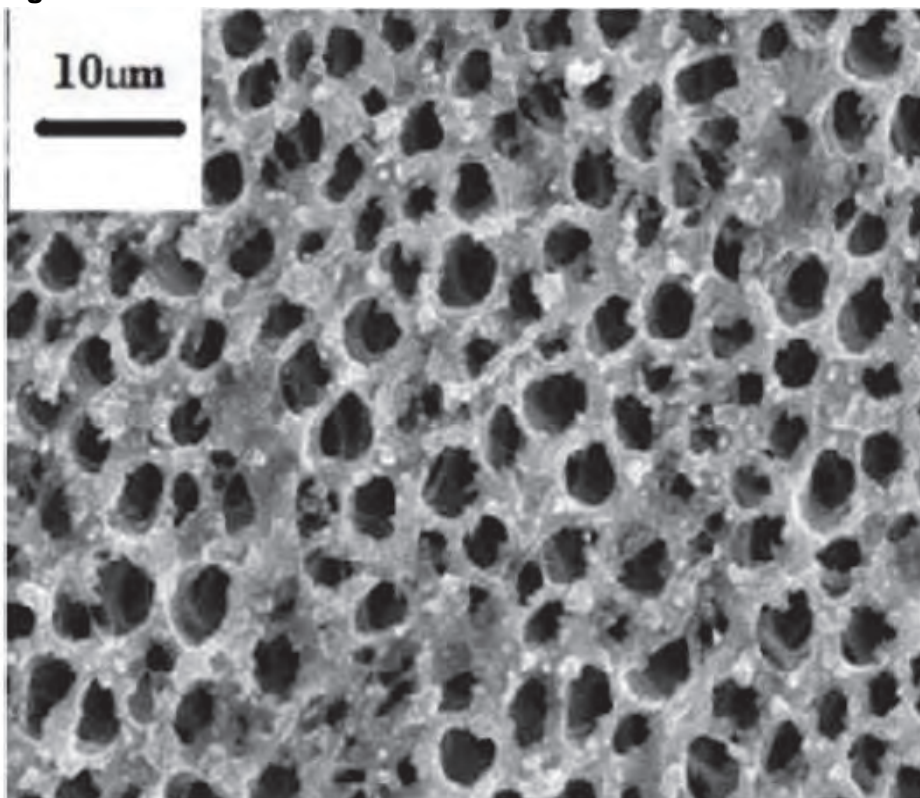


**Figure 7:** SEM of PSF/Co

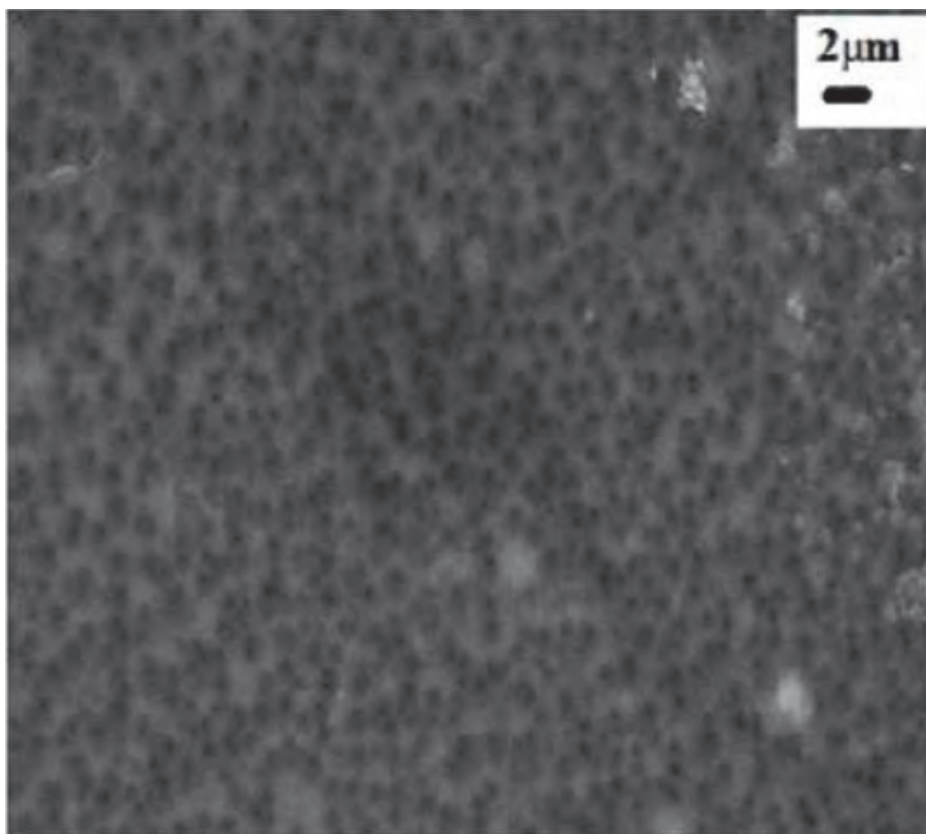


**Figure 8:** SEM of PSF/Ni

### **RAMAN spectroscopy**

In preparing for the RAMAN measurements, the PSF casting solution was drop coated on a glass slide and left to dry. All the modified casting suspensions were prepared the same as the unmodified PSF. The peak at  $1457\text{ cm}^{-1}$  is an indicative of the aromatic ring (figure 9). The Raman spectrum of PSF/Co exhibit a new peak at  $1139\text{ cm}^{-1}$  due to the symmetric C-O-C stretching mode, that was not observed in unmodified PSF (figure 10). The peak at  $1450\text{ cm}^{-1}$  indicates an aromatic ring. The peak at  $1590\text{ cm}^{-1}$  is due to the in-plane benzene ring vibration. (Xu et al. 2008). In literature reports cobalt nanocrystals were synthesized and coated onto a graphite carbon. Raman spectra indicated a peak at  $700\text{ cm}^{-1}$  due to uncoated cobalt nanoparticles. (Huang et al. 1998). The Raman spectrum of PSF/Ni exhibit a similar peak that was observed for PSF/Co at  $1141\text{ cm}^{-1}$  which indicates the symmetric C-O-C stretching mode and the in-plane benzene ring vibration peak at  $1453\text{ cm}^{-1}$  (figure 11).



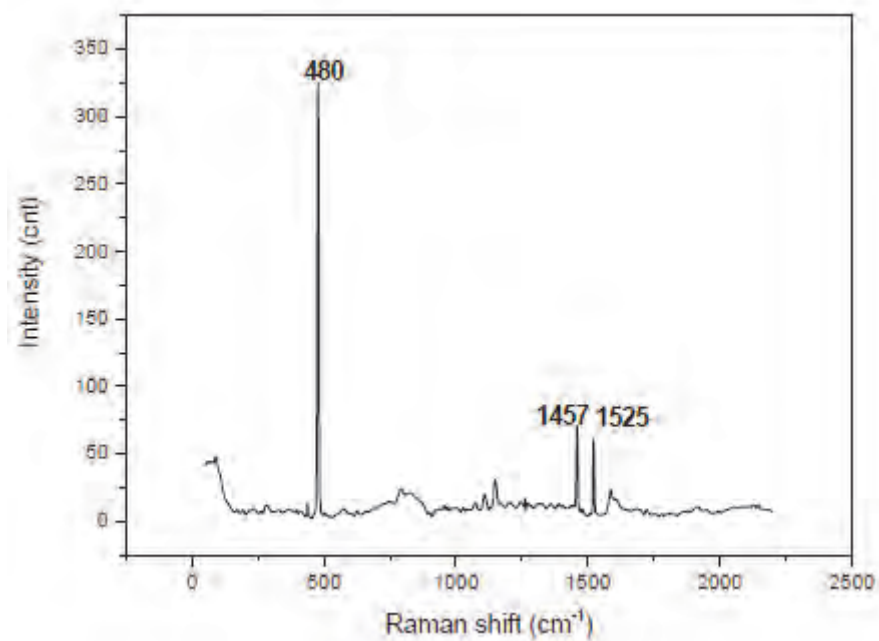


**Figure 9:** Raman spectrum of PSF

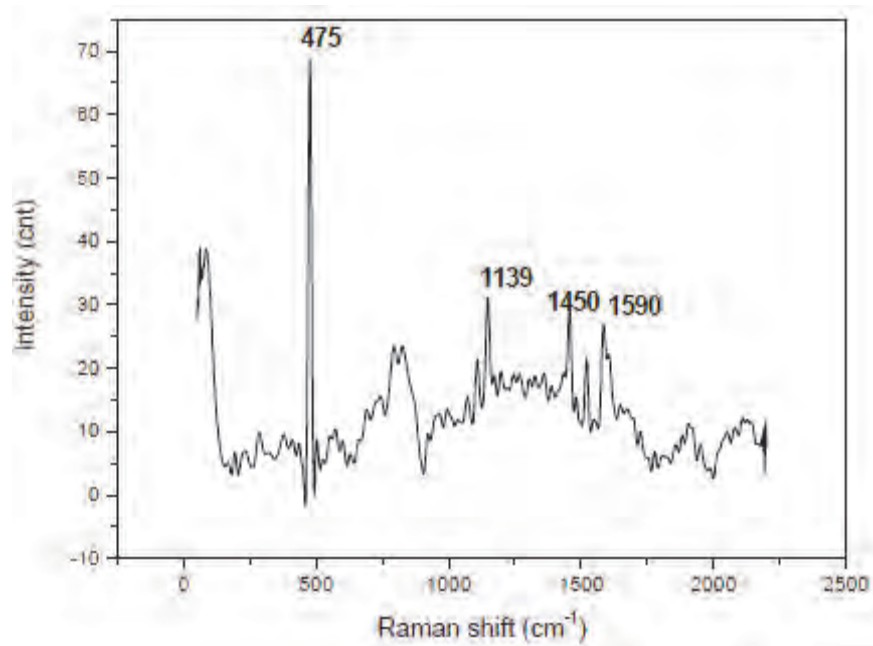


**Figure 10:** Raman spectrum of PSF/Co

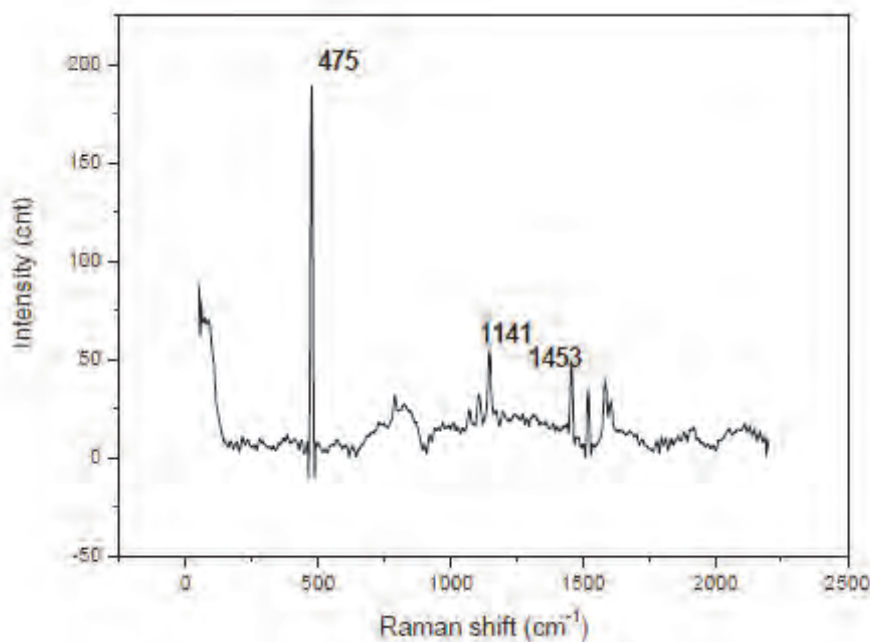


**Figure 11:** Raman spectrum of PSF/Ni

### **Synthesis of the hydrogels:**

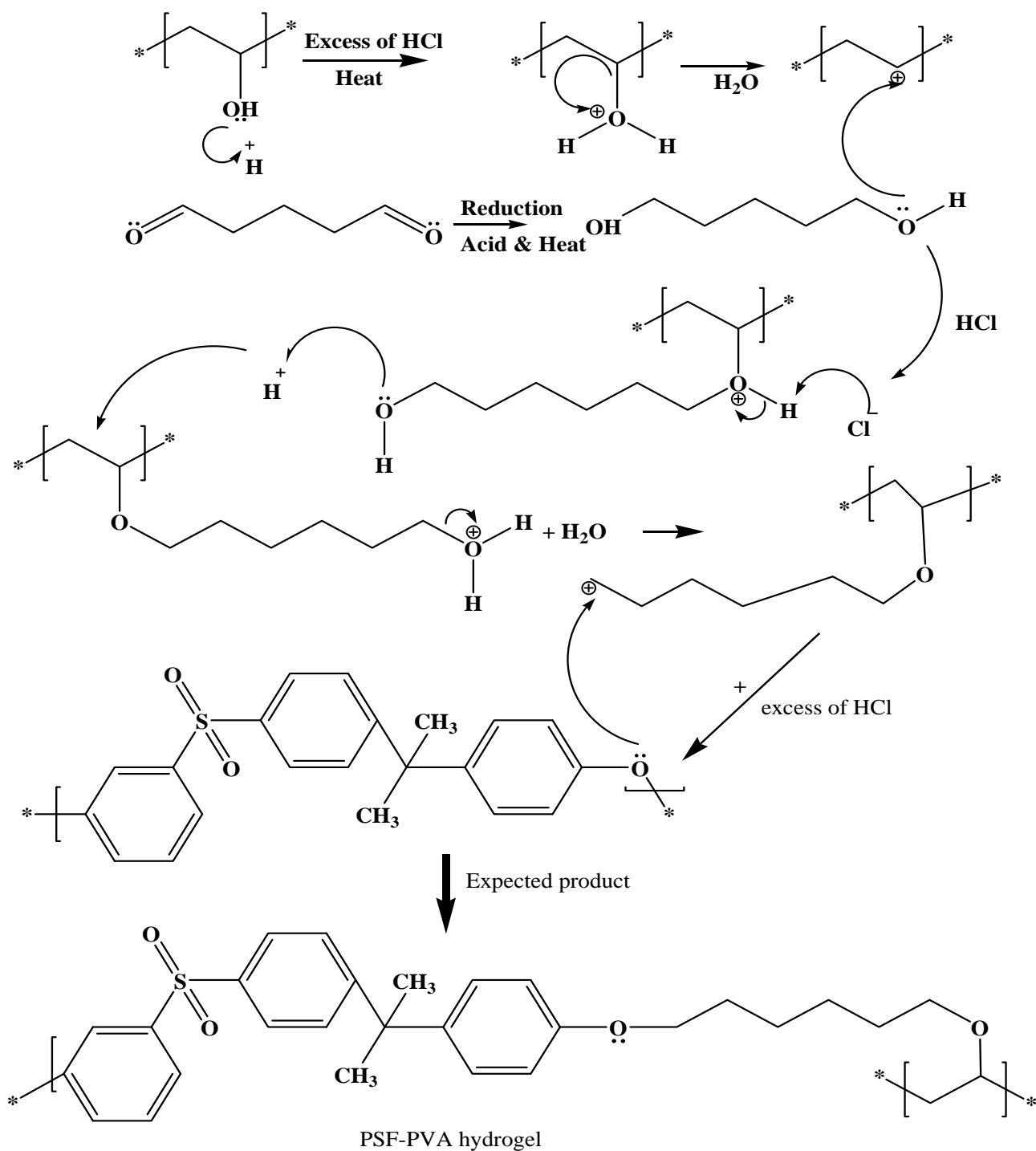
The proposed mechanism for hydrogel synthesis involved three steps:

*Steps 1:* Protonation of the alcoholic oxygen in PVA makes it a better leaving group. This step is very fast and reversible. The lone pairs of electron on the oxygen make it a Lewis base. Cleavage of the C-O bond allows for the loss of the good leaving group as a neutral water molecule, to leaving behind a primary carbocation intermediate which is very reactive. This step is the rate determining step (bond breaking endothermic).

*Steps 2:* In general reduction of an aldehyde leads to a primary alcohol.(P. Y. Bruice, (2006). Reduction of glutaraldehyde essentially involves the addition of a hydrogen atom to each end of the carbon-oxygen double bond to form an alcohol (1, 5 pentanol). This will further undergo protonation of alcoholic oxygen to form a primary carbocation.

*Steps 3:* Attack of the primary carbocation to an available oxygen site (ester or sulphone oxygen) to produce polysulfone /PVA hydrogels. (Scheme 1)

## PSF-PVA Hydrogel composite Mechanism of formation



Scheme 1 Proposed mechanism of PSF hydrogels formation

### Confirmation of crosslinking from FTIR spectroscopy

A small portion of the hydrogel was placed between two filter papers and a physical force was applied to it for dryness. The hydrogel was then dried at room temperature for 24 hours and then compressed as a KBr disk, prepared by grinding approximately 1% mixture of a

solid sample in KBr using a hydraulic press. PVA and PSF were also analysed separately and the FTIR spectrum of the pellets were recorded. The characteristic functional groups present in both PSF and PVA starting materials were identified for cross referencing in with hydrogel spectra (figure 12, 13). Analysis of functional groups in the spectra of the PSF-PVA hydrogels confirmed the cross-linking of the two polymers by the presence of the both functional groups found in PSF and PVA with a band C-H at  $3125\text{ cm}^{-1}$ , C=C at  $1800\text{ cm}^{-1}$ ,  $\text{SO}_2$  at  $1300\text{ cm}^{-1}$  and C-C at  $1100\text{ cm}^{-1}$ . The absence of OH groups from PVA was interpreted as evidence of its involvement in crosslinking (figure 14).

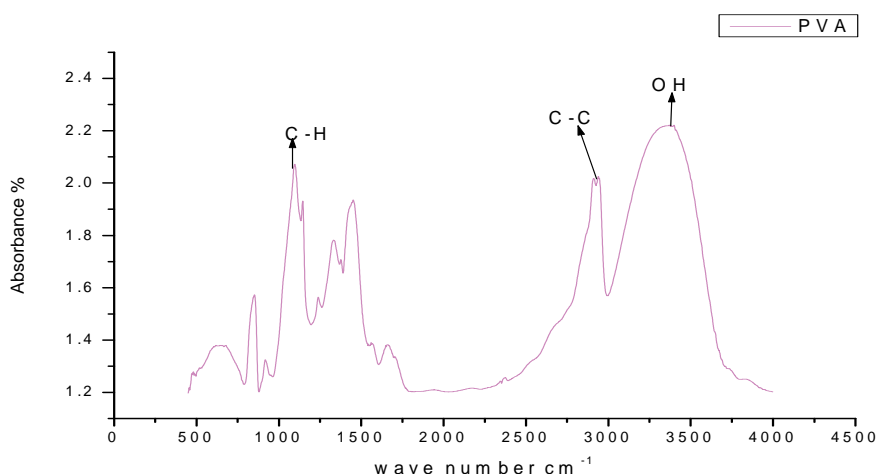


**Figure 12:** FTIR spectrum of PVA

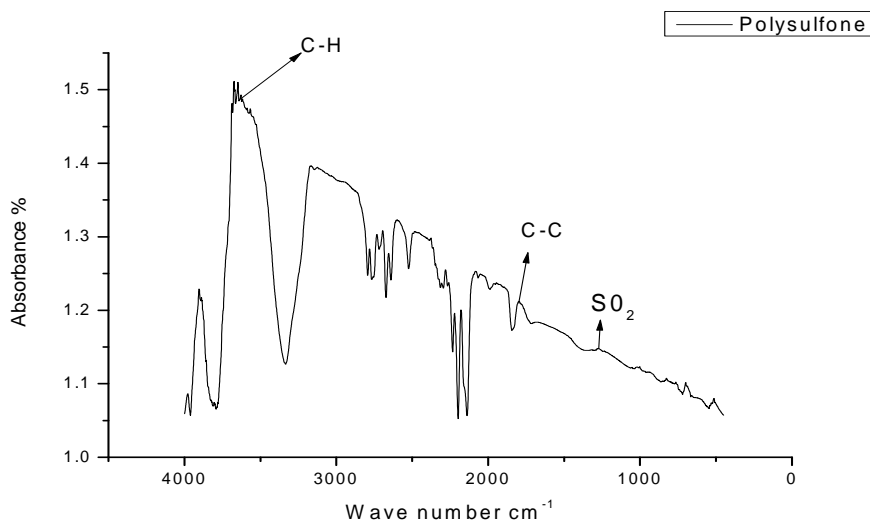


**Figure 13:** FTIR spectrum of polysulfone

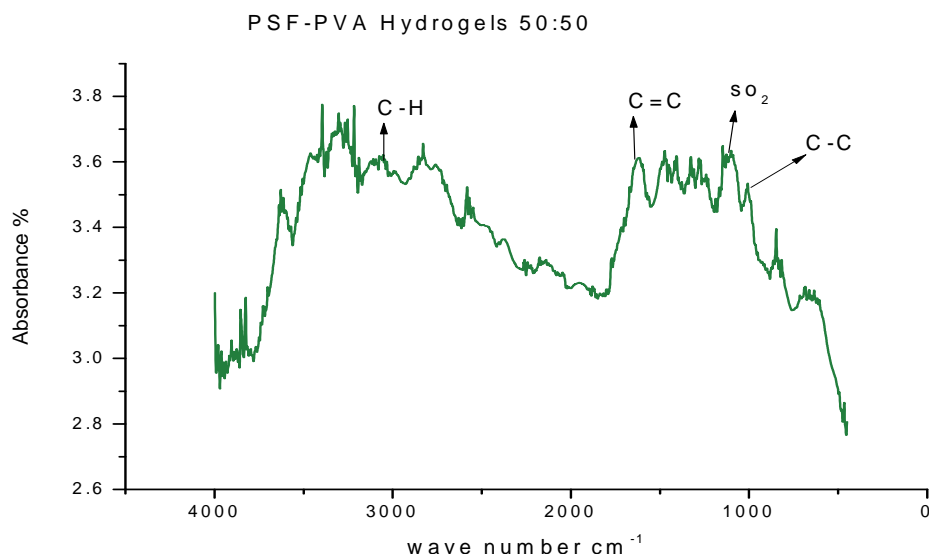


**Figure 14:** FTIR spectrum of 50:50 hydrogel

FTIR analysis provided some evidence for point of cross linkage. The spectra of the PSF-PVA hydrogels confirmed cross-linking of the two polymers by the absence C-O-C which is involved in cross linking. This indicates that the ester oxygen was the site for cross linking to form the hydrogel, since the sulphone oxygen vibrations were still visible in the spectrum of the hydrogel products

### UV/vis spectroscopy of hydrogel

The UV/vis analysis was carried out to investigate the extent of crosslinking in the hydrogels based on polysulfone absorbance parameters i.e. whether the ratio control introduced any contribution to the degree of crosslinking in hydrogels (Table 2).

**Table 2:** UV/vis analysis of hydrogel solutions

Membrane	Absorbance (A)	Wavelength
PVA	0.1	285 nm
PSF	2.8	285 nm
PSF hydrogel 50:50	1.42	275 nm
PSF hydrogel 75:25	0.53	273 nm
PSF hydrogel 25:75	0.6	273 nm

Crosslinking will produce hydrogel materials with an increase in electron density as a consequence of combined ring structures. Hence the best cross linking was observed for the 50:50 hydrogel, as indicated by the highest absorbance. Cross linking is further supported by the small shift to lower UV/vis absorbance wavelength.

### SEM of hydrogels:

Thin films were prepared as for electrochemistry by drop coating 10  $\mu\text{L}$  aliquot of PSF solution and PSF hydrogels onto screen printed carbon electrode (SPCE) with a micropipette and left to dry overnight before imaging (figure 15 1,b,c,d). Each sample was coated for viewing with gold dust to enhance the conductivity of the thin films.

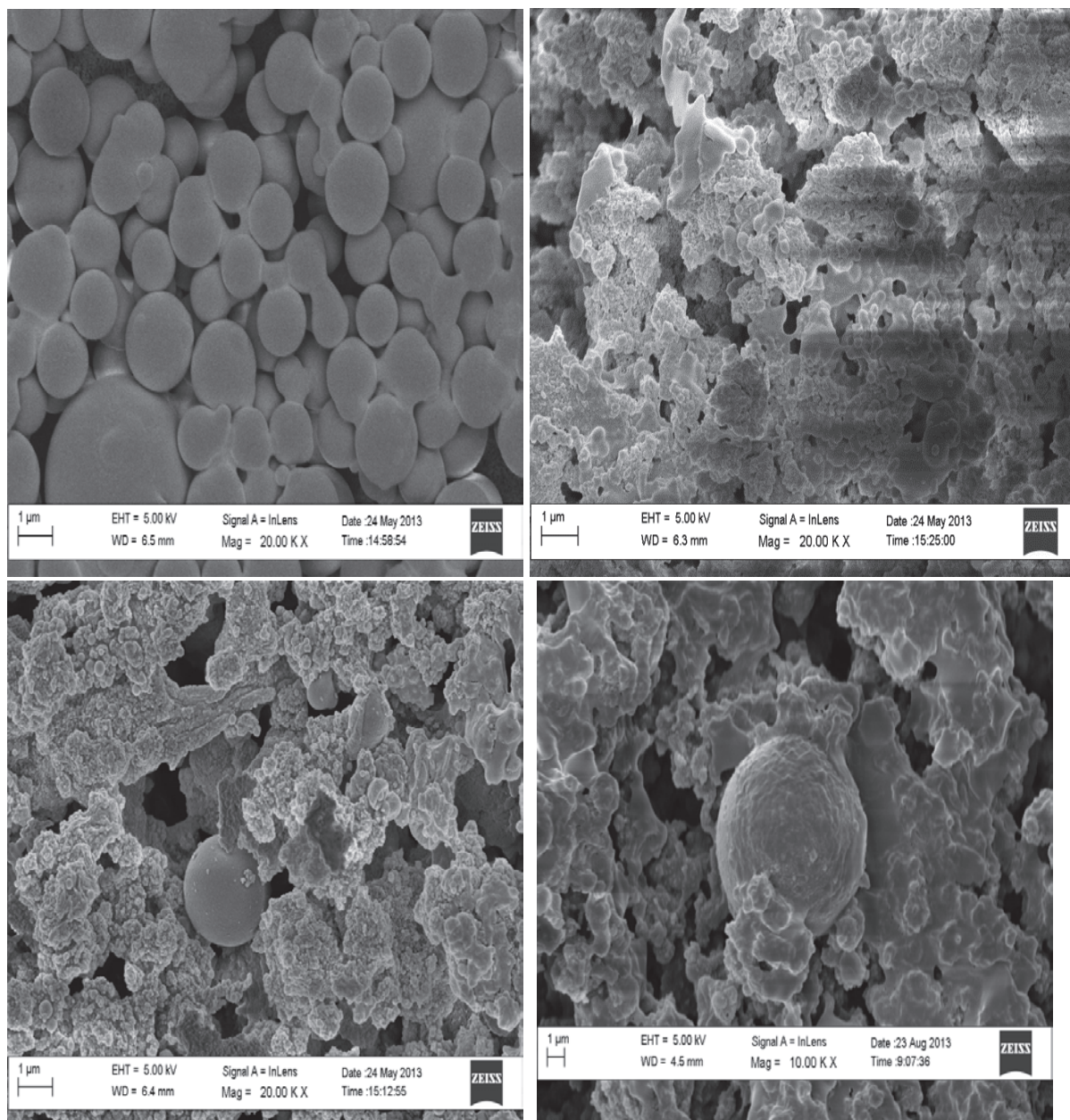


**Figure 15:** SEM of (a) PSF unmodified and (b) 50:50 hydrogel (c) 75:25 hydrogel and (d) 25:75 hydrogel.

The most effective crosslinking through chemical di-aldehyde linkage and PVA polymerisation was observed for the 50:50 hydrogel. In the experiment where PSF concentration was dominant (75:25), evidence of unreacted PSF is evident in the SEM and in the case where PVA was dominant (25:75) the PVA polymerisation appears to follow the PSF beaded template.

## AFM results

Higher surface roughness was measured for polysulfone, compared to polysulfone hydrogels (figure 16). This height distribution was in good agreement with the observed surface features of the polymers from SEM. The Sa and Ra values show a clear distribution of roughness associated with PSF contribution respectively. And a clear increase in trend upon modification with PVA was observed. Surface roughness could be associated with hydrophilicity of material. The more rough the surface the more hydrophilic it becomes. This topography trend is in good agreement with contact angle drop shape analysis and SEM images.

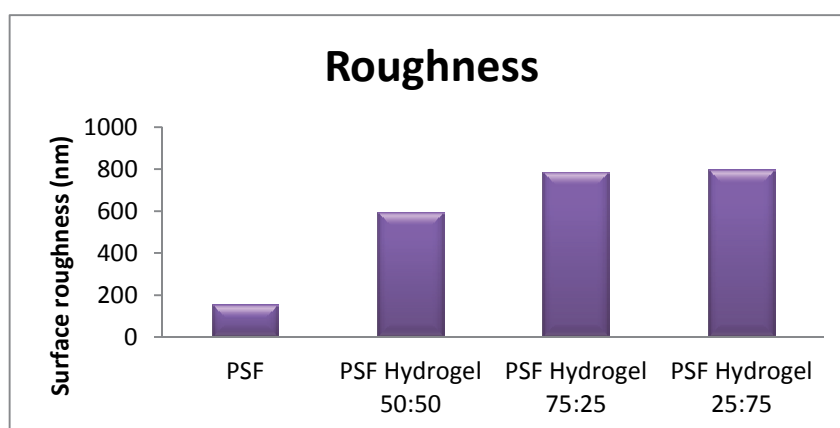


**Figure 16:** Roughness distribution as measured from AFM data

Surface roughness measurements confirmed that the dominant polymer was not as big a controlling factor as efficient crosslinking. Once cross linking was effectively achieved, the roughness as assessed by force probing, was increased dramatically.

## Contact angle measurement

Membranes are defined as hydrophobic when a contact angle greater than  $90^\circ$  is measured and hydrophilic when less than  $90^\circ$ . Unmodified polysulfone films prepared by drop coating, showed contact angles of greater than  $90^\circ$  which confirmed its hydrophobic nature. Drop shape analysis of polysulfone after chemically crosslinking with PVA, showed a decrease in contact angle by 50%. The cross linking of PVA and PSF was controlled at three different ratios to evaluate the effect of the PSF contribution i.e. 25:75, 50:50 and 75:25, but very little variation as a function of polymer ratio was observed. Polysulfone modified with metal nanoparticles (Co, Ni and Ag), showed a similar decrease in contact angle of at least 50% as a consequence of redox mediator inclusion (figure 17).



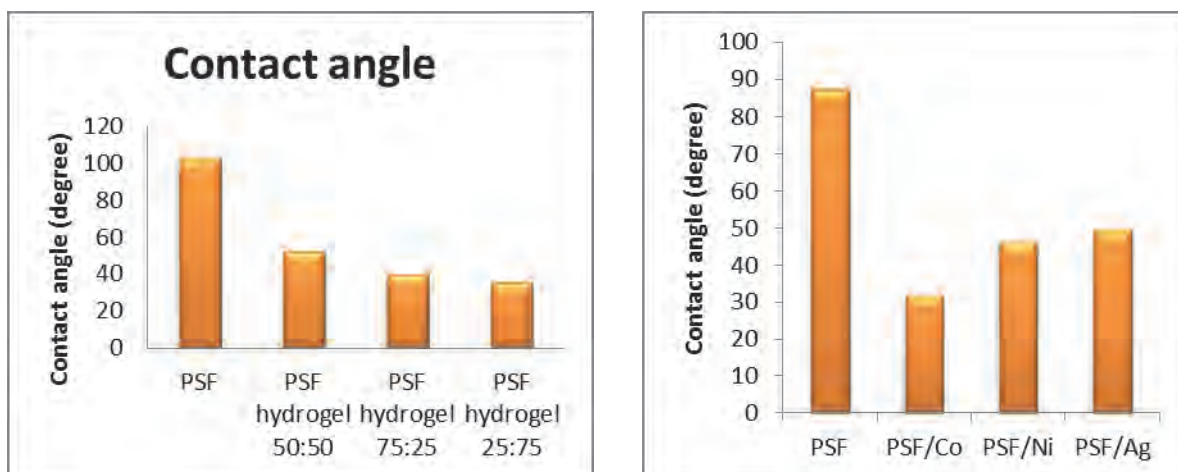


**Figure 17:** Contact angle distribution for hydrogel materials (a) as a function of polymer ratio and (b) metal nanocomposite polysulfone membranes

### Electrochemistry

Electrochemistry of polysulfone membrane materials in the presence of model compounds, alginic and tannic acid showed measureable redox performance. Redox chemistry was evaluated using cyclic voltammetry and square wave voltammetry from which kinetic parameters associated with alginic and tannic acid oxidation and reduction, was determined. Cyclic voltammetry of the polysulfone materials as thin film electrodes in the presence of varying concentration of the analyte was done to evaluate the sensitivity of the modified electrode towards analyte and calculate diffusion coefficients (figure 18, 19).

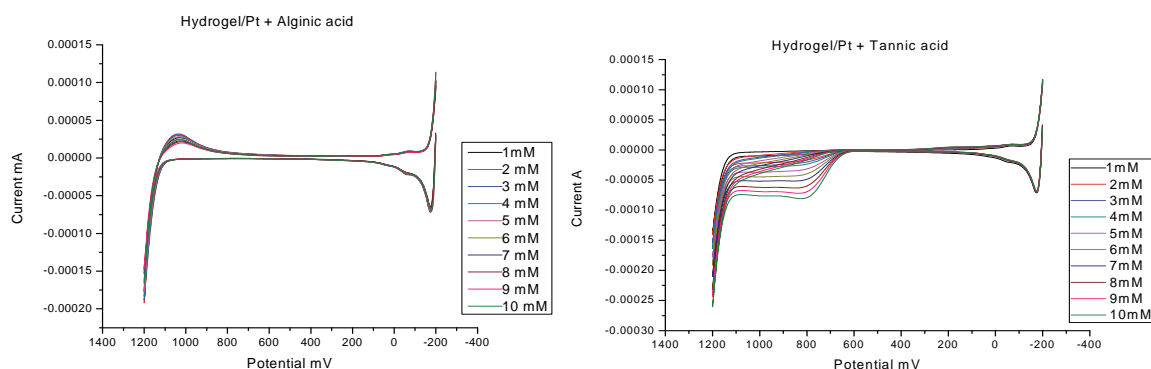


**Figure 18:** Concentration dependent response of 50:50 hydrogel in the presence of (a) alginic acid and (b) tannic acid.



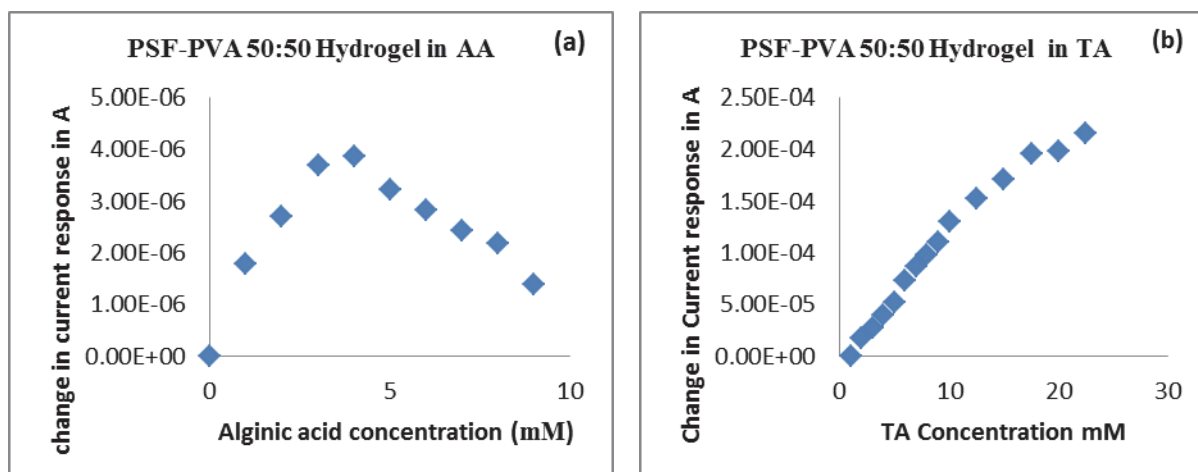


**Figure 19:** (a) Calibration curves of PSF-PVA hydrogel in the presence of (a) alginic acid, (b) tannic acid

Alginic acid did not show a unique redox peak that could be attributed to its redox chemistry, however an increase in the peak current at the Pt oxidation peak at 1100 mV (Ag/AgCl) was observed as the AA concentration was increased. This peak current response was used to construct the calibration curve for AA oxidation. Tannic acid, on the other hand showed a clearly distinguishable reductive peak at 800 mV (Ag/AgCl), which was used in the evaluation of its analytical response. From the three hydrogel composition evaluated it was evident that the hydrophilic component directly affected the diffusional properties of the thin film electrode. The highest diffusion coefficient was calculated for the 75% PVA hydrogel, although diffusion coefficients were of the same order of magnitude (Table 3). Alginic acid current response showed a decreasing trend with increasing concentration, indicative of an adsorption mechanism. Tannic acid on the other hand displayed an increasing peak current response with each addition of analyte, indicative of a catalytic reaction mechanism. In contrast to diffusion coefficient trend for the hydrogel performance, the highest sensitivity towards the analytes was measured at the 75% PSF hydrogel in each case. This indicates that both diffusional properties as well as surface physical properties, govern the analytical response of the hydrogel chemical sensors.

**Table 3:** Analytical response of polysulfone hydrogels in the presence of tannic and alginic acid

Membrane	Diffusion coefficient (Cm <sup>2</sup> /s)		Sensitivity A/mM	
	AA	TA	AA	TA
PSF	2.50 x10 <sup>-3</sup>	2,67 x10 <sup>-3</sup>	2.4 x10 <sup>-6</sup>	1.83 x10 <sup>-5</sup>
PSF/PVA 50:50	3.26 x10 <sup>-3</sup>	9.06 x10 <sup>-3</sup>	4.16 x10 <sup>-5</sup>	8.12 x10 <sup>-5</sup>
PSF-PVA 75:25	6.30 x10 <sup>-3</sup>	9.88 x10 <sup>-3</sup>	5.23 x10 <sup>-5</sup>	9,32 x10 <sup>-5</sup>
PSF-PVA 25:75	8.54 x10 <sup>-3</sup>	9.45 x10 <sup>-3</sup>	3.12 x10 <sup>-5</sup>	1,05 x10 <sup>-5</sup>

In similar experiments the analytical performance of the metal nanoparticle modified PSF materials was also evaluated.

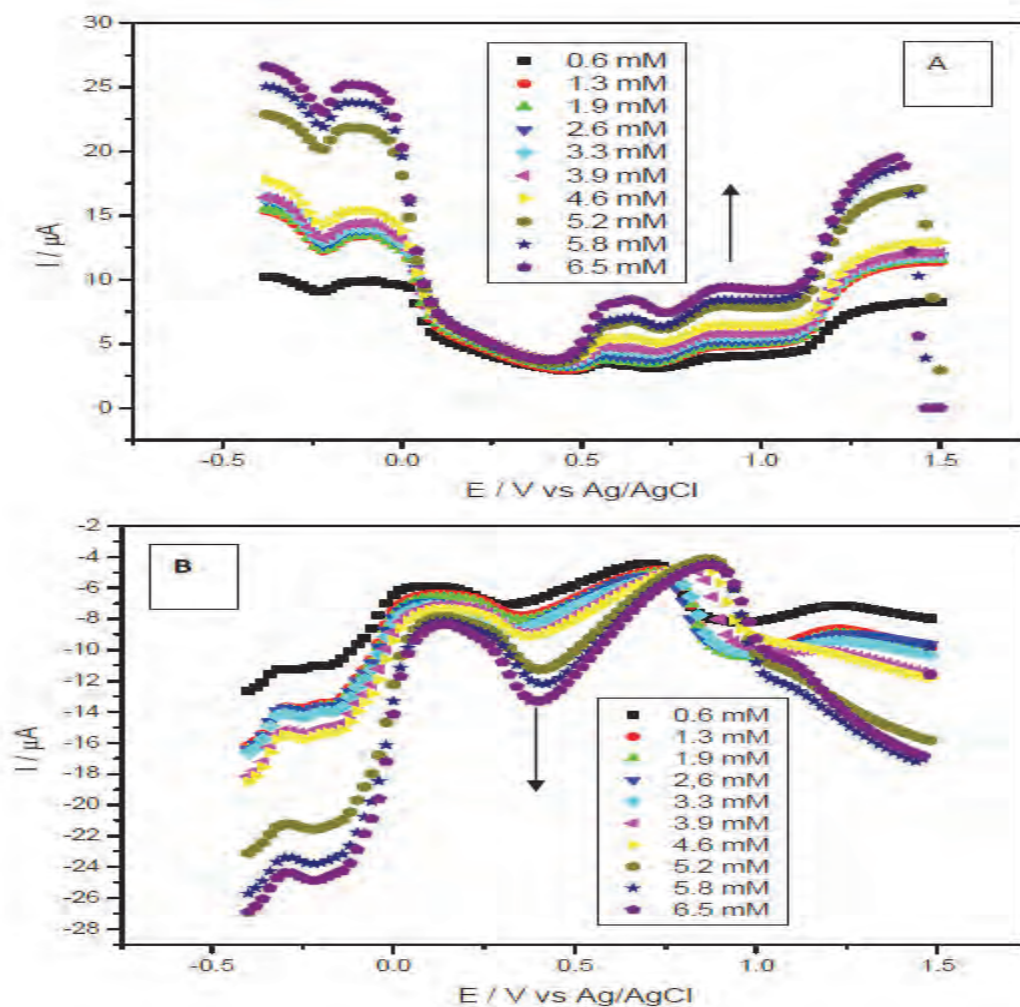


**Figure 20:** Concentration dependant SWV of PSF/Ni in the presence of tannic acid, (a) oxidation SWV and (b) reduction SWV

Nanoparticle modified PSF square wave current response to increasing alginic acid concentration in solution showed a decreasing peak current response as measured at -400 to +1500 mV (vs Ag/Ag/Cl) also observed for hydrogel sensors, whereas tannic acid redox current response as measured at -200 to +1200 mV mV (vs Ag/Ag/Cl) showed an increasing redox current response (figure 20). The analytical current response was selected as the peak showing the most distinguishable change after each addition, even though the electrochemistry of the Pt/PSF interface was dominated by background Pt electrochemistry in HCl electrolyte

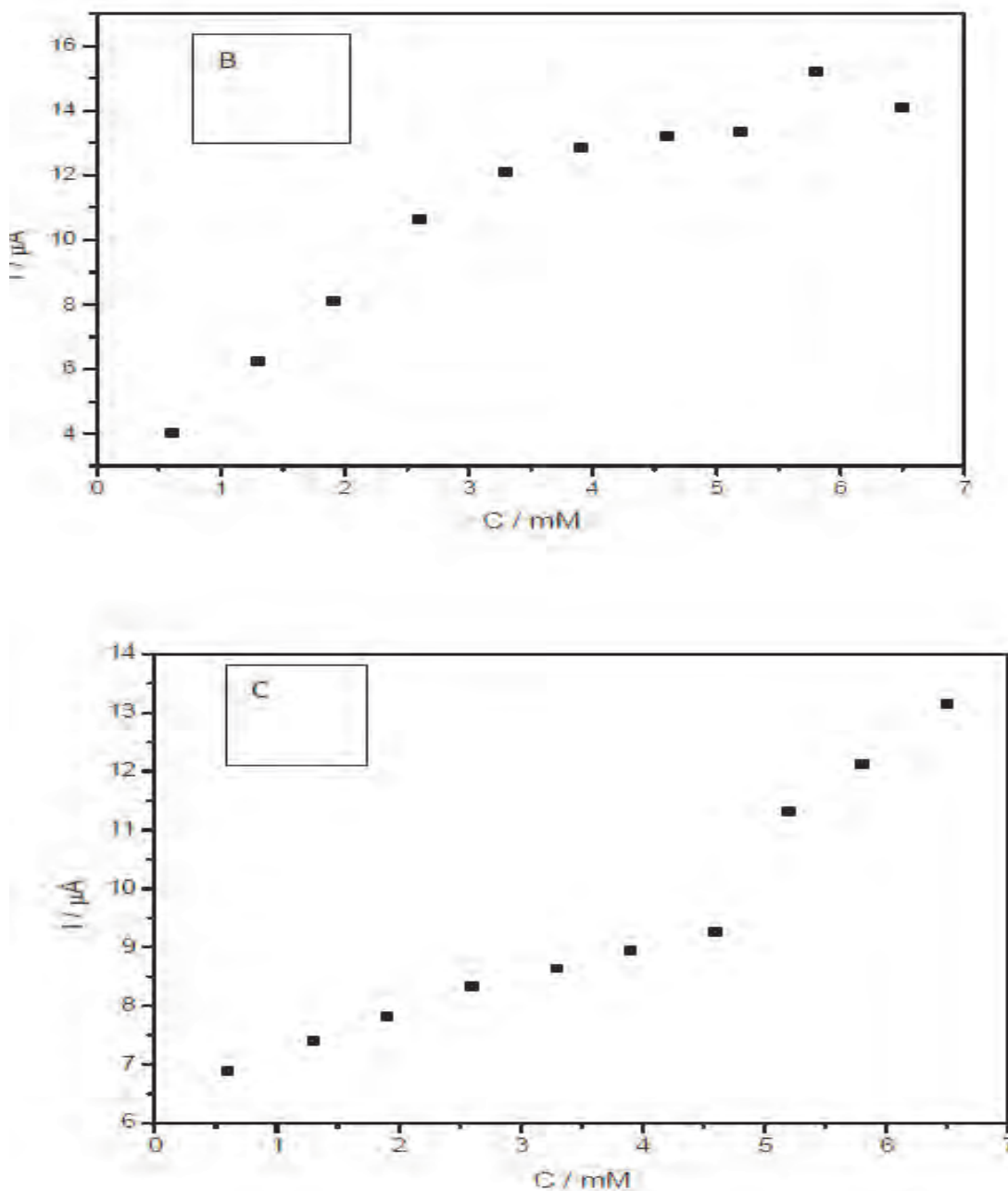


**Figure 21:** Calibration Curves for (b) Pt/PSF/Co (c) Pt/PSF/Ni in the presence of tannic acid.

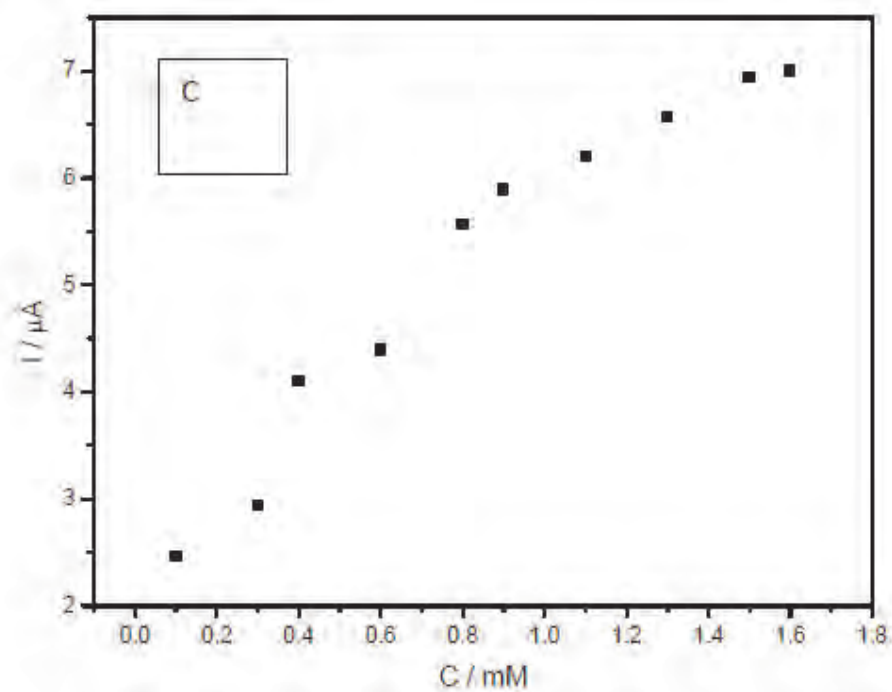
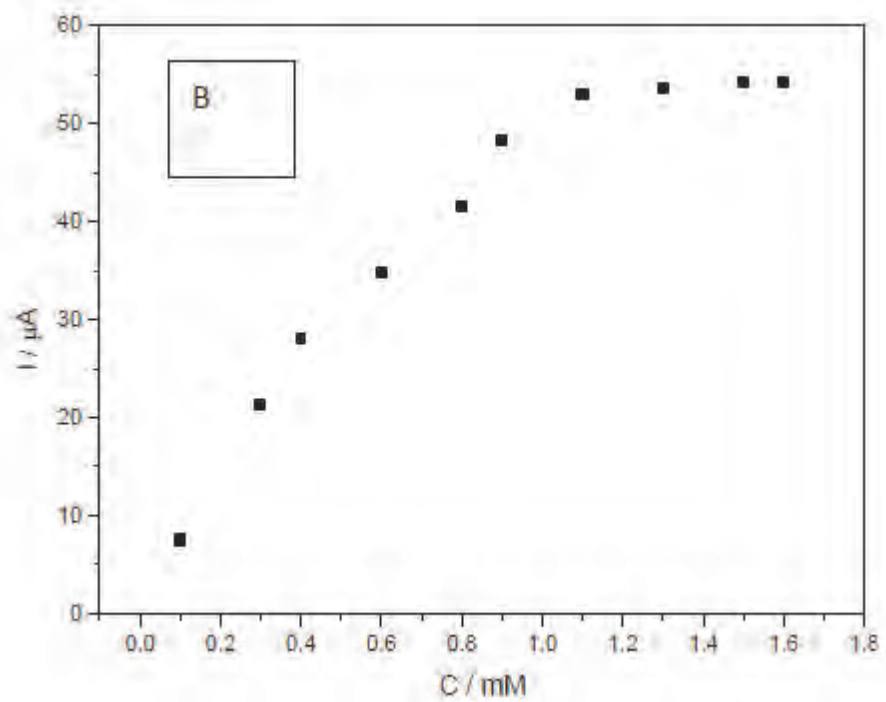


**Figure 22:** Calibration Curves for (b) Pt/PSF/Co (c) Pt/PSF/Ni in the presence of alginic acid.

**Table 4:** Comparison of PSF, and PSF modified with nanoparticles in the presence of tannic and alginic acid

Membrane	Diffusion coefficient (Cm <sup>2</sup> /s)		Sensitivity A/mM	
	AA	TA	AA	TA
PSF	$2.50 \times 10^{-3}$	$2.67 \times 10^{-3}$	$2.41 \times 10^{-6}$	$1.83 \times 10^{-5}$
PSF-Co	$1.29 \times 10^{-3}$	$2.85 \times 10^{-3}$	$4.46 \times 10^{-6}$	$3.06 \times 10^{-5}$
PSF-Ni	$3.20 \times 10^{-3}$	$2.55 \times 10^{-3}$	$3.03 \times 10^{-5}$	$4.01 \times 10^{-6}$
PSF-Ag	$4.63 \times 10^{-3}$	$3.43 \times 10^{-3}$	$1.22 \times 10^{-5}$	$1.09 \times 10^{-5}$

The calibration curves were constructed from SWV data for polysulfone nano composites membrane material (figure 21). Polysulfone membranes modified with cobalt, silver and nickel behaved as a chemical sensor for the redox electrochemistry of tannic acid and alginic acid in aqueous solution, with negligible shift in peak potential as a function of concentration. Comparable to PSF hydrogels the diffusion coefficients were all calculated to be of the same order of magnitude, with the Ag nanoparticle modified polysulfone registering the highest diffusion coefficient in the presence of tannic acid and alginic acid respectively. PSF/Ni showed the highest sensitivity towards alginic acid whereas as PSF/Co showed the highest sensitivity towards tannic acid, as measured from the slope of the calibration curves (Table 4).

### Electrochemical Impedance spectroscopy (EIS)

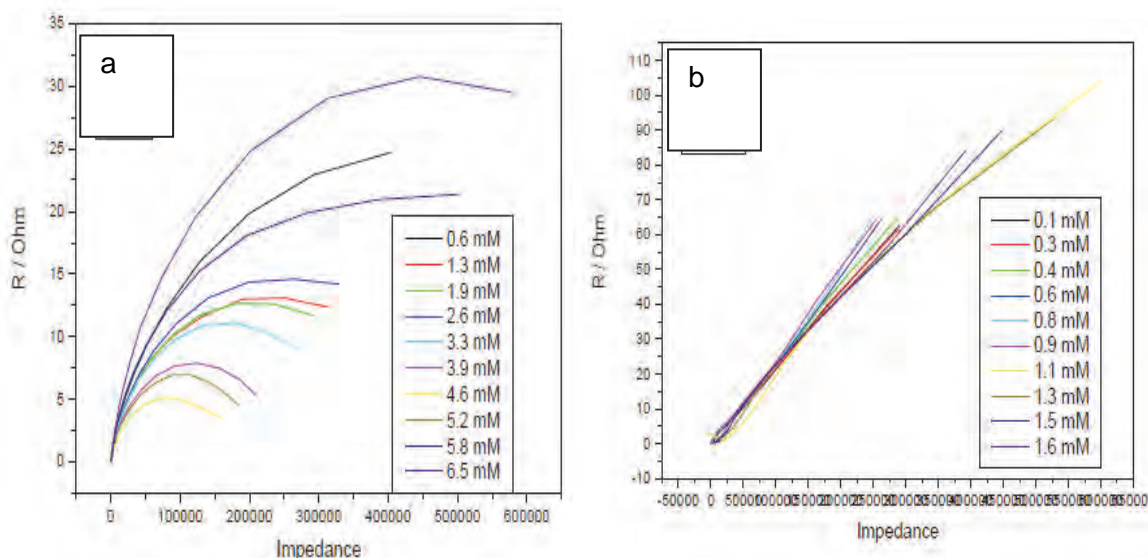


**Figure 23:** (A) PSF/Ni in the presence of tannic acid, (B) PSF/Ni in the presence of alginic acid

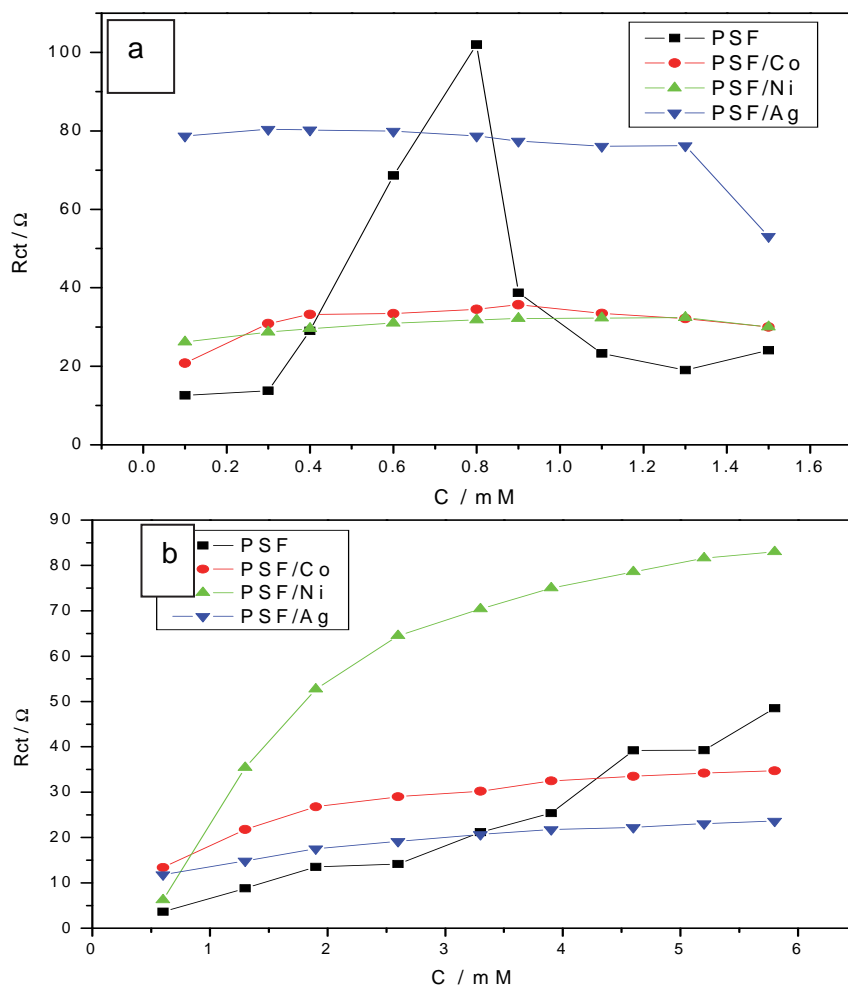


**Figure 24:** Calibration curves of Polysulfone nanocomposite in (a) alginate acid and (b) tannic acid

The electrochemical impedance response of the metal nanoparticle modified PSF in the presence of tannic acid evaluated at 0.58 V (figure 22). The PSF/Ni films showed the best quantitative response indicated by the limit of detection which was 2.6 mM, and highest sensitivity towards tannic acid indicated by the highest slope which was found to be  $2.91 \times 10^{-6} \Omega / \text{mM}$  (figure 23). However all films showed a tendency towards fouling above 2 mM of tannic acid added.

The PSF unmodified was inconsistent in its response to alginate acid and may require further controlled evaluation. However the same inconsistency in concentration response was also observed in voltammetric evaluation (CV, SWV).

The same experiment was also conducted for PSF-PVA hydrogels materials. Tannic acid at fixed potential of 0.58 V and over a frequency of 100 mHz to 1 KHz was evaluated as concentration dependent response. The electrocatalysis of TA followed typical diffusion control kinetics as evidenced by semi-circle at low frequency in the concentration range evaluated and was modelled as Randles circuit using CPE to model non-homogenous

adsorption at the interface. Alginate acid electrocatalysis at fixed potential of 0.37 V and over a frequency range of 100 mHz to 1 KHz was evaluated as a concentration dependent response. Alginate acid electrocatalysis appeared to be influenced by passivating infinite diffusive behaviour as evidenced by unresolved low frequency impedance arcs. This type of data should best be modelled as infinite Warburg diffusion, but for consistency in data interpretation, the same RCT circuit was used as for tannic acid.

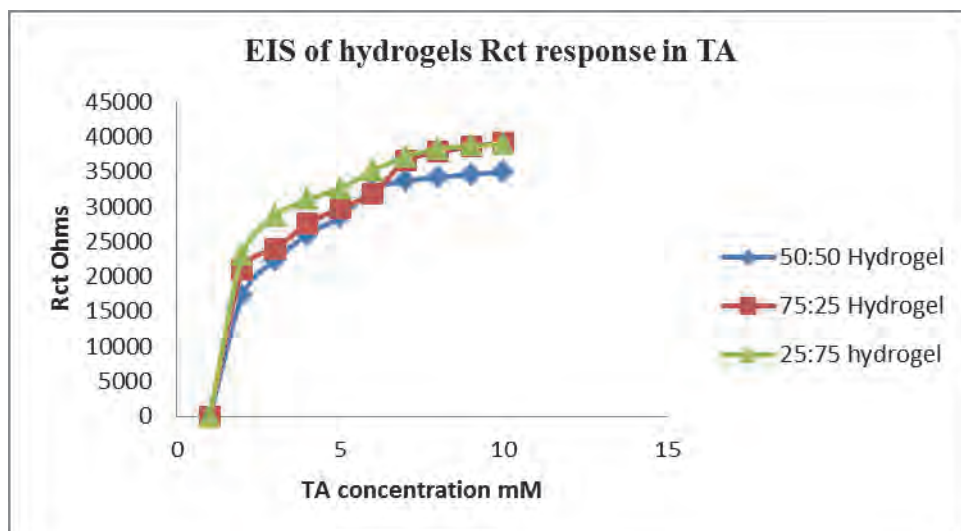


**Figure 25:** Calibration curves PSF-hydrogel in tannic acid

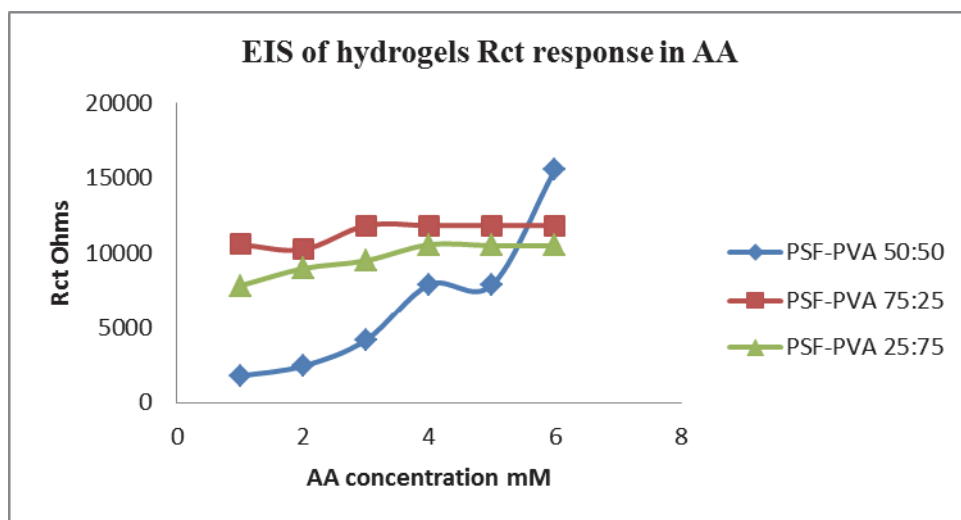


**Figure 26:** Calibration curves PSF-hydrogel in alginate acid

The impedance data was modelled as equivalent electrical circuits for the quantitative evaluation of charge transfer and capacitance behaviour. The hydrogel interface was observed to increase in conductivity (decrease in Rct) due to the charging effect of the applied analytical potential, but still facilitated a linear response to tannic acid concentration (figure 24). No major change in the interfacial capacitance was expected, since the tannic acid oxidation was electrocatalytical driven and indeed the change in capacitance remains fairly constant until limit of detection had been reached. The corresponding impedance trend



expected for an adsorptive mechanism would be an increase in  $R_{ct}$  and an increase in capacitance as the adsorbed analyte material increased the interfacial charge separation and slowed down electron transfer kinetics. However the concentration dependent impedance showed no trend as a function of concentration, either increasing or decreasing and remained fairly constant in both parameters over the concentration range evaluated (figure 25).

Commonly used methods for quantification of alginates are based on a preliminary enzymatic depolymerization, and/or chemical hydrolysis of alginate to release simple carbohydrates to be detected by colorimetric methods or chromatographic methods. HPLC has emerged as the main method of detection for oligosaccharides such as alginates with retention times typically between 10-20 minutes. The analysis involves derivatising the alginates using suitable enzymes followed by fractional analysis, which is both time consuming and costly (Yan Liu et al. 2000; Hanan Awad et al. 2012). Tannic acid may be analyzed by a variety of methods including spectrophotometry, titration, liquid chromatography and protein-precipitation method. However the simple methods suffer from inadequate sensitivity, whereas the more complex methods require expensive instrumentation (Yu-Gang Sun et al. 2000). The polysulfone chemical sensors developed in this work offer a rapid and simple detection method for alginic acid and tannic acid, with comparable sensitivity to flow injection analysis method ( $2 \times 10^{-8}$  mol/l) (Liang We et al. 2010). Polysulfones have been applied in the development of different types of sensors including humidity sensors, gas sensors and biosensors. Immunosensors based on polysulfone as matrix, graphene oxide as electrochemical transducer and model rabbit antibody (RlgG) as bio-recognition element have been previously demonstrated in literature (Samuel Sanchez Ordonez et al. 2007)

Modification of PSF with Co, Ni and Ag nanoparticles reduces hydrophobicity by (~40 %) and modification by crosslinking with PVA produced a stable hydrogel material with reduced hydrophobicity (~50%) and reproducible electrochemistry even under hydrodynamic conditions (rotating disk electrochemistry not shown). All hydrophilic polysulfones displayed high sensitivity to the small organic molecules evaluated at the micromole concentration range. As individual analytes the selected model compounds produced clearly distinguishable electrochemistry responses that may be further developed to produce robust chemical sensors for application in aqueous environment. The consistency in diffusion coefficient magnitude could be related to reduced hydrophobicity and holds promise for the development of highly stable electrochemical platforms in the development of biosensors, immunosensors and genosensors.

### **Preliminary assessment of fouling behaviour based on laboratory scale small volume experiments.**

#### **(i) Fixed frequency diffusion behaviour**

For a Hydrophobic interface we expect a weak approach to the electrode interface and the capacitance of the interfacial region will be small. As the analyte molecules are brought to the surface of the electrode during convection, the presence of the analyte will manifest as an increase in capacitance of the interface over longer time (figure 27a). At a hydrophilic membrane, the approach of the analyte molecule will be easily facilitated and a change in



capacitance should be visible at an earlier onset time and the capacitance should also be large as many molecules approach the interfacial region (figure 27b). The magnitude of the interfacial capacitance will be determined by the size of the analyte molecule and the available active electrode surface area.

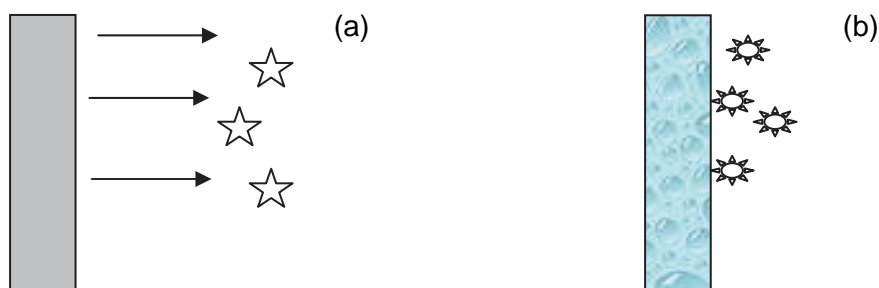


**Figure 27:** (a) hydrophobic membrane interface (b) hydrophilic membrane interface

Fixed Frequency EIS studies were done at fixed frequency of 10 Hz in the presence of tannic acid and alginic acid (figure 28). The low frequency impedance of PSF/Ni and PSF/Co materials in the presence of a fixed concentration of the analyte was measured at very low potentials. The low frequency range was chosen to represent the area where diffusion behaviour could be best observed and the low potentials were chosen to avoid electrochemical induced analytic behaviour

The capacitance response range for PSF was measured as 0.7  $\mu\text{F}$  to 1.2  $\mu\text{F}$  Farads. The time at which the capacitance decay reaches a plateau was evaluated as the onset of fouling. For a hydrophilic interface the time should be comparatively shorter. For PSF/Ni and PSF/Co comparatively shorter approach times for tannic acid and alginic acid approach was measured. As noted before, different mechanisms of reaction were identified for the two model compounds and they also have different stereochemistry. Both of these factors would affect the final diffusional behaviour. However it is noteworthy that under controlled conditions favouring predominantly diffusional behaviour and for identical experiments, differentiation in onset of fouling as defined here) was measurable using interfacial capacitance evaluated from EIS data as analytical parameter.

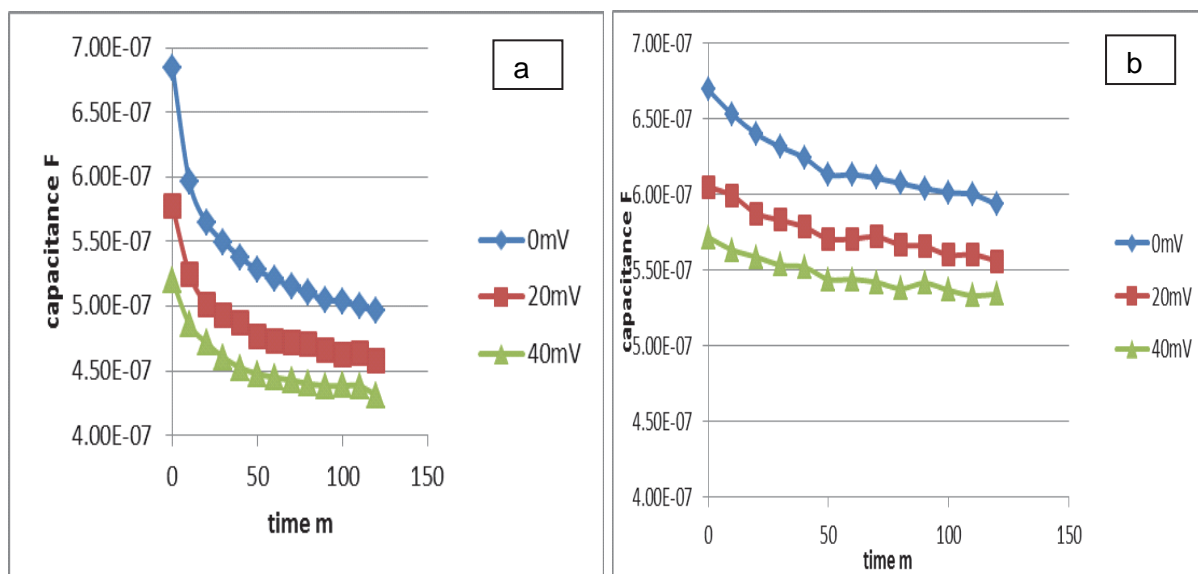


**Figure 28:** Fixed frequency EIS studies for PSF/Ni in the presence of (a) alginate acid and (b) tannic acid

**Table 5:** Polysulfone thin films prepared in the presence of tannic acid and alginate

Material	Slope ( F/m)	Standard Deviation (F/m)	Cut-off time (m)
Polysulfone	Alginate acid $3.25 \times 10^{-9}$	$5.68 \times 10^{-9}$	44
	Tannic acid $6.31 \times 10^{-9}$	$1.80 \times 10^{-9}$	46
Polysulfone/Co	Alginate acid $1.80 \times 10^{-9}$	$4.32 \times 10^{-9}$	35
	Tannic acid $2.07 \times 10^{-9}$	$1.93 \times 10^{-9}$	27
Polysulfone/Ni	Alginate acid $7.53 \times 10^{-1}$	$2.2 \times 10^{-9}$	39
	Tannic acid $3.49 \times 10^{-9}$	$1.55 \times 10^{-8}$	42

#### Impedance measurements using real sludge samples:

Suitable sludge samples were obtained from South African Breweries (SAB, Western Cape) containing microbes that they culture themselves, for the brewing process. Sludge samples may contain typical acidogens/acetogens already present in the wastewater such as *Clostridium* (producing acetone, butanol), *Acetobacter* (acetic acid), *Escherichia* (mixed acids) and *Propionibacterium* (propionate). Exact populations will differ from one situation to the next. Fixed frequency impedance analysis of the polysulfone materials in the presence of the sludge and with consistent stirring was measured as a function of time (figure 29). During this study (PhD, 2011) the cellulose acetate hydrophilic membrane was also available

for comparison of its performance under the same conditions. The hydrophilic membranes clearly showed a higher rise in total impedance (largely capacitive, since no potential control was applied and system was kept as open circuit) as well as marginally shorter onset of impedance increase, as compared to the hydrophobic membranes. However due to unknown composition and concentration of the microbial sludge we were not able to quantify the fouling behaviour in any way. These experiments were repeated over time and similar trends were observed.

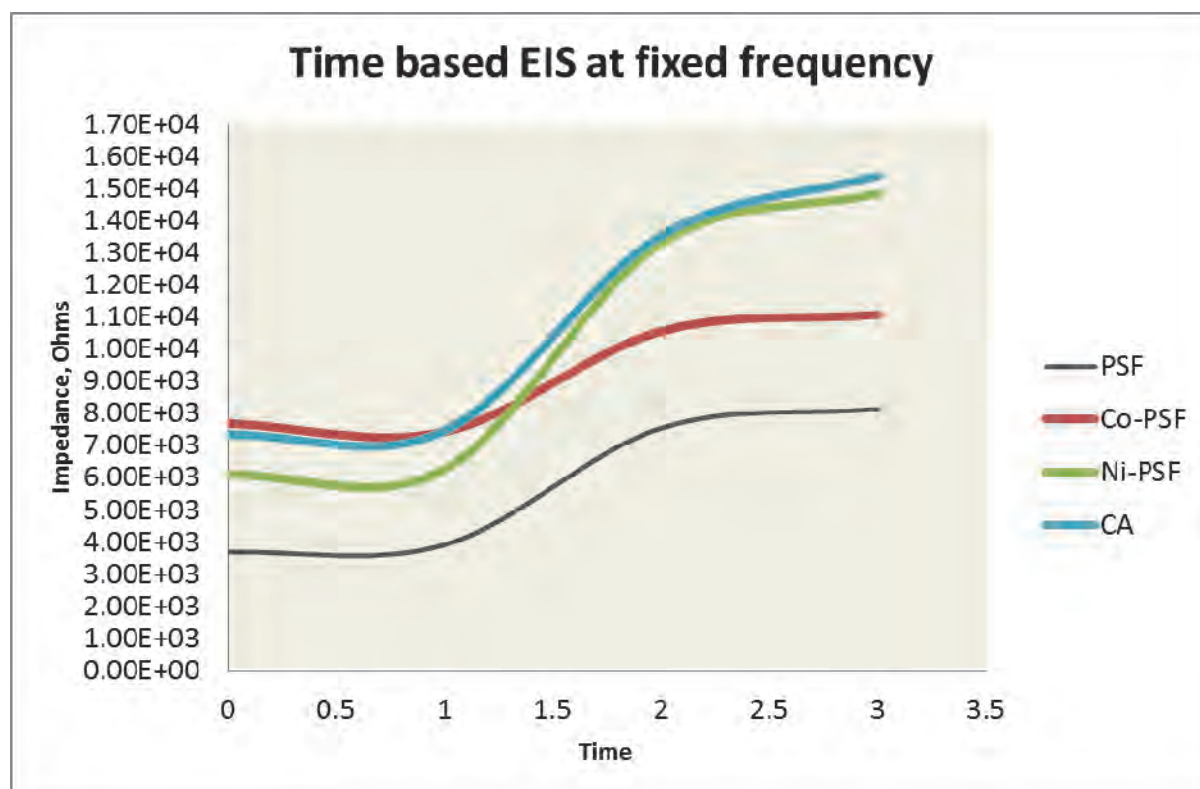


**Figure 29:** Fixed frequency Impedance of microbial sludge (SAB)

However both these experiments as well as concentration dependent analytical response support the theoretical model proposed in this research for evaluating fouling behaviour as a function of interfacial impedance measured as either capacitance (for diffusional controlled reaction) or charge transfer resistance (for faradaic response) in the presence of defined reaction conditions such as concentration and reaction mechanisms of chemical species.

## 5 CONCLUSIONS

The preparation of polysulfone membranes modified with selected catalytic metal nanoparticles was successfully achieved. The polysulfone composite based on homogeneous incorporation of Ni nanoparticles, before film casting, was observed to have the smallest pore size and highest pore distribution per unit area. The Ni nanoparticles adopted the hexagonally close packed unit arrangement with packing efficiency up to 74%. In the analytical evaluation of PSF/Ni composites drop coated to form thin film chemical sensors, a very good sensitivity towards tannic acid and alginic acid was observed with a linear response in the micro molar concentration range.

One of the drawbacks of using metal nanoparticles in environmental applications relates to potential environmental health related issues as a result of metal nanoparticles leaching into the environment. Hence a second synthetic approach was evaluated that does not involve metal nanoparticles, based on chemical crosslinking of polysulfone with a hydrophilic polymer to produce mechanically stable hydrophilic hydrogels. Polysulfone and polyvinyl alcohol were chemically cross linked using a short chain di-aldehyde to produce hydrogels with greatly reduced hydrophobicity, irrespective of the ratio of the starting polymers. All hydrogels showed similarities to the metal nanoparticle modified polysulfone in terms of surface morphology and electrochemical evaluation of mass transport properties to the thin film hydrogel surface in a three electrode arrangement. All hydrogel materials showed very good sensitivity and linear response to tannic acid and alginic acid at micro molar concentrations.

Overall the project has been successful in achieving all its objectives for materials design, development and testing at a laboratory scale. The project has provided skills training and expertise in advanced analytical methods for 1 PhD, 2 MSc and 2 Honours full time registered candidates (UWC). The data produced in this project has resulted in 3 peer reviewed publications in international scientific journals (already accepted) and a 4<sup>th</sup> full length research article submitted for peer review (February 2014).

## **6 RECOMMENDATIONS**

The research results show great promise for the utilisation of hydrophilic polysulfone derivatives for improved separation efficiency in aqueous media, as a direct consequence of reduced hydrophobicity at the interface of these membrane materials. The results at laboratory scale, small volume experiments bode well for efficient separation of polysaccharides and carbohydrates, as demonstrated by alginic acid and tannic acid response, respectively. It was demonstrated that alginic acid (polysaccharides) through adsorption mechanism posed a greater threat to membrane fouling as compared to tannic acid (carbohydrates). The research has also convincingly positioned electrochemistry as a reliable analytical technique for the evaluation of flux to membrane surfaces.

However to verify the fouling behaviour, a series of scaled up experiments are necessary. The feasibility of casting flat membrane sheets using the polysulfone (Ni) and polysulfone cross linked with PVA (75:25) would have to be evaluated. The separation efficiency of these two membranes in a small volume flow through reaction cell has to be evaluated. The scaling up of the flow through volume would have to be evaluated as a function of membrane mechanical stability and separation efficiency.

Thereafter it is necessary to evaluate the membrane performance in a small scale membrane reactor using simulated separation mixtures as well as real organic membrane reactor feed solutions. This type of reaction vessel will facilitate evaluation of the efficiency of the membrane in the presence of physical foulants (sludge) and facilitate the evaluation of regenerating membranes *in situ*, using cost efficient regeneration processes. Electrochemical measurements and modelling of processes within the small scale membrane bioreactor will facilitate the demonstration of electrochemistry as an efficient analytical tool for the evaluation of flux through a membrane as well, following a well-developed literature precedent.

## 7 LIST OF REFERENCES

- Awad, H., Aboul-Enein, H. Y. (2012) "Validated HPLC Assay Method for the Determination of Sodium Alginate in Pharmaceutical Formulations", *Journal of Chromatographic Science*, pp 1-7.
- Bae, T. & Tak, T. (2005) "Effect of TiO<sub>2</sub> nanoparticles on fouling mitigation of ultrafiltration membranes for activated sludge filtration", *Journal of Membrane Science*, vol. 249, no. 1-2, pp. 1-8.
- Bruice, P.Y. (2006). *Essential organic chemistry*, (6<sup>th</sup> Edition). International Standard Book Number (ISBN): -13: 978-0321663139
- Chen, S., Liou, R., Lai, C., Hung, M., Tsai, M., Huang, S. (2008) "Embedded nano-iron polysulfone membrane for dehydration of the ethanol/water mixtures by pervaporation", *Desalination*, vol. 234, no. 1-3, pp. 221-231.
- Fan, Z., Wang, Z., Duan, M., Wang J. and Wang, S. *Journal of membrane science*, 310 (2008) 402-408
- Fan, Z.F., Wang, Z., Sun, N., Wang, J.X., Wang, S. C. Performance improvement of polysulfone ultrafiltration membrane by blending with polyaniline nanofibers, *Journal of membrane Science*. 320 (2008), pp 363-371.
- Gang Sun, Y., Hua, C., Li, Y.H., Zhao, H.Z., Lin. X.Q. (2000) "Flow Injection Analysis of Tannic Acid with Inhibited Electro-chemi-luminescent Detection". *Analytical Letters*, 33 (2000), pp 2281-2291
- Howell, J.A., Sanchez, V., Field, R.W. (1993) *Membranes in Bioprocessing: Theory and Application*, Chapman & Hall, Cambridge, UK.
- Ju, H., McCloskey, B.D., Sagle, A.C., Kusuma, V.A., Freeman, B.D. (2009) "Preparation and characterization of cross linked ploy(ethylene glycol) diacrylate hydrogels as fouling-resistant membrane coating materials.", *Journal of Environmental Sciences*, vol. 330, pp. 180-188.
- Kim, J., Van der Bruggen, J. (2010) "The use of nanoparticles in polymeric and ceramic membrane structures: Review of manufacturing procedures and performance improvement for water treatment", *Environmental Pollution*, vol. 158, no. 7, pp. 2335-2349.
- Kweon, J.H., Lawler, D.F. (2005) "Investigation of membrane fouling in ultrafiltration using model organic compounds". *Water Sci Technol*. 51(6-7), pp101-6.
- Maximous, N., Nakhla, G., Wan, W. (2010) "Performance of a novel ZrO<sub>2</sub>/PES membrane for wastewater filtration". *J. Membr. Sci.*, 352, pp. 222-230.
- Maximous, N., Nakhla, G., Wan.W. (2009) "Comparative assessment of hydrophobic and hydrophilic membrane fouling in wastewater applications", *Journal of Membrane Science*, vol. 339, no. 1-2, pp. 93-99.
- Nomura, T., Fujii, T., Suzuki, M. (1997) "Application of the ceramic membrane with hydrophobic skin layer to separation of activated sludge". *Water Science and technology*, vol. 35, pp. 137.
- Omidian, H., Rocca, J.G., Park, K. (2005) "Advances in superporous hydrogels", *Journal of Controlled Release*, vol. 102, pp. 3-12.
- Owino, J.H.O., Omotayo, A., Baker, P.G.L., Guiseppi-Elie, A and Iwuoha, E. (2008). "Synthesis and characterisation of poly (2-hydroxylethyl methacrylate) polyaniline based hydrogel composites". *Journal on reactive & functional polymers* 68, pp 1239-1244.
- Sagle,A.C., Ju, H., Freeman, B.D., Sharma, M.M. (2009) "PEG-based hydrogel membrane coatings", *Polymer*, vol. 50, pp. 756-766.

- S. Sanchez Ordonez, E. Fabregas. (2007) "New antibodies immobilization system into a graphite-polysulfone membrane for amperometric immunosensors." *Biosensors and Bioelectronics* 22, pp 965-972.
- E.H Schacht, (2004). Polymer chemistry and hydrogel system, *Journal of Physics: Conference Series*. 3 22
- H. Susanto, M. Ulbricht, (2008) "High-performance thin layer hydrogel composite membranes for ultrafiltration of natural organic matter". *Journal on water research* 42 (2008) 2827-2835
- Q. Sun, Y. Su, X. Ma, Y. Wang, Z. Jiang. (2006) "Improved antifouling property of zwitterionic ultrafiltration membrane composed of acrylonitrile and sulfobetaine copolymer." *Membrane Science*, vol. 285, pp. 299-305.
- K.H. Syed, G. S. Al-Assaf, G. O Phillips. (2011). *Hydrogels: Methods of preparation, characterisation and Applications*. International Standard Book Number (ISBN) 978-953-307-268-5 .
- L. Wei. (2010) "Online Determination of Trace Amounts of Tannic Acid in Colored Tannery wastewaters by Automatic Reference Flow Injection Analysis." *Journal of Automated Methods and Management in Chemistry*, Article ID 920196, pp 1-4.
- L.Yan, J. Xiao-Lu, C. He , G. Hua-Shi. (2000) "Analysis of oligomannuronic acids and oligoguluronic acids by high-performance anion-exchange chromatography and electrospray ionization mass spectrometry". *Journal of Chromatography A*, 884, pp 105-111.
- Y. Yanan, Z. Huixuan, W. Peng, Z. Qingzhu, L. Jun. ( 2007) "The influence of nano-sized TiO<sub>2</sub> fillers on the morphologies and properties of PSF UF membrane", *Journal of Membrane Science*, vol. 288, pp. 231-238.
- H. Yu, M. Hu, Z.K. Xu, J. Wang, S. Wang. (2005) "Surface modification of polypropylene microporous membranes to improve their antifouling property in MBR:NH<sub>3</sub> plasma treatment.", *Separation and Purification Technology*, vol. 45, pp. 8-15.
- K. Zodrow, L. Brunet, S. Mahendra, D. Li, A. Zhang, Q. Li, P.J.J. Alvarez. (2009) "Polysulfone ultrafiltration membranes impregnated with silver nanoparticles show improved biofouling resistance and virus removal.", *Water Research*, , pp. 715.

## APPENDIX

**Table A1:** Diffusion coefficients ( $\text{cm}^2/\text{s}$ ) calculated for polysulfones in 0.5 M  $\text{H}_2\text{SO}_4$  and PBS (pH=7.2) and using  $\text{K}_3\text{Fe}(\text{CN})_6$  as redox probe.

	PSF	Co-PSF	Ni-PSF
$\text{H}_2\text{SO}_4$	$6.85 \times 10^{-4} \text{ cm}^2/\text{s}$	No peaks	$1.11 \times 10^{-3} \text{ cm}^2/\text{s}$
$\text{H}_2\text{SO}_4 + \text{K}_3\text{Fe}(\text{CN})_6$	$1.41 \times 10^{-8} \text{ cm}^2/\text{s}$	$1.54 \times 10^{-8} \text{ cm}^2/\text{s}$	$4.19 \times 10^{-8} \text{ cm}^2/\text{s}$
PBS	$1.64 \times 10^{-3} \text{ cm}^2/\text{s}$	$1.64 \times 10^{-3} \text{ cm}^2/\text{s}$	$1.61 \times 10^{-3} \text{ cm}^2/\text{s}$
PBS+ $\text{K}_3\text{Fe}(\text{CN})_6$	$1.06 \times 10^{-8} \text{ cm}^2/\text{s}$	$1.12 \times 10^{-9} \text{ cm}^2/\text{s}$	$1.53 \times 10^{-8} \text{ cm}^2/\text{s}$

**Table A2:** Diffusion coefficients ( $\text{cm}^2/\text{s}$ ) calculated under hydrodynamic conditions for polysulfones in 0.5 M  $\text{H}_2\text{SO}_4$  and PBS (pH=7.2) and using  $\text{K}_3\text{Fe}(\text{CN})_6$  as redox probe.

	PSF	Co-PSF	Ni-PSF
$\text{H}_2\text{SO}_4$	$1.04 \times 10^{-4} \text{ cm}^2/\text{s}$	$2.51 \times 10^{-5} \text{ cm}^2/\text{s}$	$3.71 \times 10^{-4} \text{ cm}^2/\text{s}$
$\text{H}_2\text{SO}_4 + \text{K}_3\text{Fe}(\text{CN})_6$	$5.75 \times 10^{-8} \text{ cm}^2/\text{s}$	$7.80 \times 10^{-9} \text{ cm}^2/\text{s}$	$2.01 \times 10^{-7} \text{ cm}^2/\text{s}$
PBS	$2.70 \times 10^{-3} \text{ cm}^2/\text{s}$	$6.49 \times 10^{-3} \text{ cm}^2/\text{s}$	$6.52 \times 10^{-4} \text{ cm}^2/\text{s}$
PBS+ $\text{K}_3\text{Fe}(\text{CN})_6$	$1.52 \times 10^{-7} \text{ cm}^2/\text{s}$	$3.18 \times 10^{-8} \text{ cm}^2/\text{s}$	$8.35 \times 10^{-8} \text{ cm}^2/\text{s}$

**Table A3:** Contact angle measurements of metal nanoparticle modified PSF thin films.

Material	Mean Contact angle ( $^\circ$ ) (n=4, STD <20%)
Polysulfone (PSF)	87.5
Cobalt-polysulfone (Co-PSF)	31.7
Nickel-polysulfone (Ni-PSF)	46.19
Cellulose acetate (CA)	42.6
Polyethersulfone (PES)	53.0

### Wetting experiments

t = time taken for drop of water to be absorbed by material

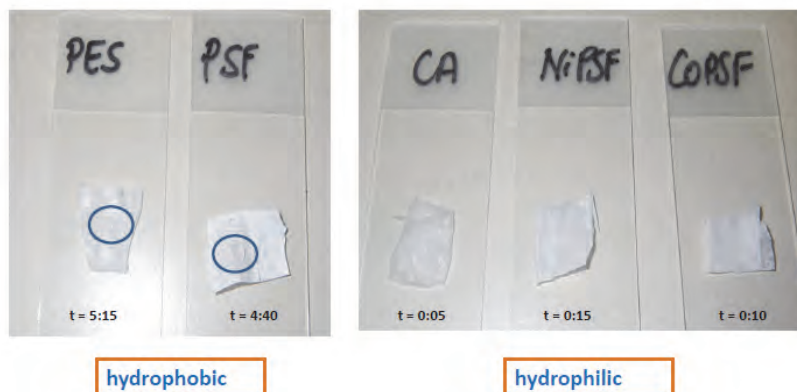


**Figure A1:** Wetting experiments for commercial and novel polysulfone composite films

**Table A4:** Comparison of PSF, PVA and PSF hydrogels electrochemistry in HCl.

Membrane	Diffusion coefficient ( $\text{Cm}^2/\text{s}$ )		Formal potential (mV) $\Delta E^\circ$	$I_{pc}/I_{pa}$
	Oxidation	Reduction		
PSF	$3.625\text{e}^{-12}$	$8.1563\text{e}^{-12}$	439.6	0.446
PVA	$1.450\text{e}^{-9}$	$3.2625\text{e}^{-9}$	211.0	1.68
PSF/PVA 50:50	$3.260\text{e}^{-11}$	$9.06\text{e}^{-9}$	431.25	1.81
PSF/PVA 75:25	$6.3251\text{e}^{-10}$	$9.8541\text{e}^{-8}$	575.85	1.52
PSF/PVA 25:75	$8.5428\text{e}^{-10}$	$9.458\text{e}^{-8}$	410.5	1.84

**Table A5:** Comparison of surface analysis with diffusion coefficient.

Hydrogels	Contact angle	Roughness (nm)	Diffusion coefficient	
			$D_o \text{ Cm}^2/\text{s}$	$D_R \text{ Cm}^2/\text{s}$
PSF:PVA 50:50	52°	595.6	$3.211\text{e}^{-11}$	$9.06\text{e}^{-9}$
PSF:PVA 75:25	40°	786.8	$6.32\text{e}^{-10}$	$9.88\text{e}^{-8}$
PSF:PVA 25:75	36°	789.9	$8.54\text{e}^{-10}$	$9.45\text{e}^{-8}$

**Table A6:** Analytical performance of hydrogels in the presence of alginate acid.

Membrane	Sensitivity	LOD	$R^2$
Hydrogel 25:75	$3\text{e}^{-05}\text{A}/\mu\text{M}$	6 $\mu\text{M}$	0.98807
Hydrogel 50:50	$2.\text{e}^{-6}\text{A}/\mu\text{M}$	5 $\mu\text{M}$	0.97047
Hydrogel 75:25	$5\text{e}^{-05}\text{A}/\mu\text{M}$	6 $\mu\text{M}$	0.9843



**Table A7:** Analytical performance of hydrogels in the presence of tannic acid.

Membrane	Sensitivity	LOD	R <sup>2</sup>
Hydrogel 25:75	1e-05A/ $\mu$ M	20 $\mu$ M	0.9748
Hydrogel 50:50	8e-5A/ $\mu$ M	20 $\mu$ M	0.9937
Hydrogel 75:25	9e-05A/ $\mu$ M	18 $\mu$ M	0.9644

**Table A8:** Analytical performance of hydrogels under hydrodynamic conditions.

Membrane	TA & AA concentration range $\mu$ M	Sensitivity
PSF hydrogel 25:75	(1-6 ) $\mu$ M	TA = 0.0214 A/ $\mu$ M AA = 0.0231 A/ $\mu$ M
PSF hydrogel 50:50	(1-8 ) $\mu$ M	TA = 0.0225 A/ $\mu$ M AA = 0.0128 A/ $\mu$ M
PSF hydrogel 75:25	(1-6 ) $\mu$ M	TA = 0.5935 A/ $\mu$ M AA = 0.3526 A/ $\mu$ M